Paleogene climate dynamics in the Primorye Region, Far East of Russia, based on a Coexistence Approach analysis of palaeobotanical data

Olesya V. Bondarenko, Nadezhda I. Blokhina, Volker Mosbrugger & Torsten Utescher

Palaeobiodiversity and Palaeoenvironments

ISSN 1867-1594
Volume 100
Number 1

Palaeobio Palaeoenv (2020) 100:5-31
DOI 10.1007/s12549-019-00377-4

Springer

Palaeobiodiversity and Palaeoenvironments (2020) 100:5–31
https://doi.org/10.1007/s12549-019-00377-4

SENCKENBERG

ORIGINAL PAPER

Paleogene climate dynamics in the Primorye Region, Far East of Russia, based on a Coexistence Approach analysis of palaeobotanical data

Olesya V. Bondarenko[1] · Nadezhda I. Blokhina[1] · Volker Mosbrugger[2] · Torsten Utescher[2,3]

Received: 13 July 2018 / Revised: 17 September 2018 / Accepted: 26 February 2019 / Published online: 21 May 2019

Abstract

The Paleogene climate dynamics in Primorye (Far East of Russia) are studied using the Coexistence Approach, based on palaeobotanical records. Palaeobotanical data for the reconstruction comprises 54 palaeofloras covering the early Paleocene to late Oligocene, a time span of ca. 42 myr. The climate inferences obtained are consistent with independently derived global trends, demonstrating general climate cooling through the Paleogene. Cooling is most striking regarding the cold month mean temperature, while the decline of mean annual temperature was less marked. Our data indicate that the Paleogene climate of Primorye was significantly warmer than present, in general, with the warmest conditions prevailing throughout the Eocene and in the southeast of the study area. Negligible Paleogene temperature gradients over Primorye are related to the global pattern and specific regional aspects. The precipitation reconstruction points to conditions considerably wetter than at present. A distinct increase in mean annual precipitation is observed for the early Eocene and persisted throughout the Eocene and Oligocene. The regional rainfall pattern fundamentally differed from modern conditions, and this holds for all studied variables. The inland region and the south of Primorye were significantly more humid than today. The Paleogene pattern was possibly related to a monsoon-type circulation and enhanced landward flow of humid air masses, due to an overall flatter geomorphology of the East Asian coastal areas.

Keywords Climate seasonality · Monsoon intensity · Precipitation pattern · Spatial gradients · Temperature evolution · Temporal trends

✉ Nadezhda I. Blokhina
blokhina@biosoil.ru

Olesya V. Bondarenko
laricioxylon@gmail.com

Volker Mosbrugger
volker.mosbrugger@senckenberg.de

Torsten Utescher
t.utescher@uni-bonn.de

[1] Federal Scientific Center of the East Asia Terrestrial Biodiversity, Far Eastern Branch, Russian Academy of Sciences, Prospect Stoletiya 159, Vladivostok 690022, Russia

[2] Senckenberg Research Institute and Natural Museum, Senckenberganlage 25, 60325 Frankfurt M., Germany

[3] Steinmann Institute, University of Bonn, Nussallee 8, 53115 Bonn, Germany

Introduction

The Paleogene (65.5–23.03 Ma) globally was an interval of significant climatic and biotic reorganisation (Akhmetiev 2004). It was a period of climate changes from greenhouse to icehouse conditions in the so-called doubthouse times marked by climatic cooling, rapid growth of the Antarctic ice sheet and a supposed drop in atmospheric CO_2 levels leading to the Eocene–Oligocene Transition (EOT) event (Pagani et al. 2005; Dupont-Nivet et al. 2007; Eldrett et al. 2009; Pearson et al. 2009; Xiao et al. 2010; Abels et al. 2011).

Two examples of global climatic events have been identified in the Paleogene: the first is a warming trend in the late Paleocene–early Eocene time that began in the middle of Paleocene, the second is a cooling trend that set on near the end of the middle Eocene and continued to the late Oligocene. The hyperthermal Paleocene–Eocene Thermal Maximum (PETM) event displays the highest temperature in the Cenozoic (Zachos et al. 2008). Thus, after a relatively stable Paleocene,

followed by warming throughout the early Eocene, and punctuated by the PETM, at 55.5 Ma, global temperatures underwent a long-term decreasing trend that culminates in the current icehouse climate mode (Zachos et al. 2008; Bijl et al. 2009).

The knowledge of the climate evolution during the Paleogene provides unique perspectives for the modeling of actual global changes and helps to probe into the integrated response of the Earth system to various driving forces (Zachos et al. 2008; Utescher et al. 2009).

The Primorye Region (or Primorye) is located in the south of the Russian Far East (RFE), on the coast of the Sea of Japan, bordering the Eurasian continent and Pacific Ocean (Gerasimov 1969). Located in the transitional zone 'continent-ocean', this territory constantly experiences the influence of oceanic-atmospheric and continental-atmospheric events. The study of the climate evolution of Primorye in the geological past, in particular in the Paleogene, promotes the understanding of the formation of modern climate in this region.

Case studies of geological records offer direct evidence to explain the palaeoclimatic changes. The evolution of Paleogene climates in eastern Eurasia in general and Primorye in particular is tied to the history of the East Asian Monsoon (EAM) and is complicated by tectonic events such as uplift of the Tibetan Plateau, and the Sea of Japan back-arc opening (e.g. An et al. 2001; Liu and Yin 2002; Akhmetiev 2004, 2015; Sato et al. 2006; Yamamoto and Hoang 2009; Pavlyutkin and Golozubov 2010; Quan et al. 2012; Liu et al. 2015; Tada et al. 2016; Akhmetiev and Zaporozhets 2017). Moreover, past climates of eastern Eurasia are supposed to reflect the varying intensity of the warm Kuroshio and cold subarctic currents (e.g. Gallagher et al. 2009; Matthiessen et al. 2009).

Paleogene regional climates can be reconstructed from the palaeobotanical records with a different degree of reliability, depending on the spatio-temporal resolution of palaeobotanical sites, and the taxonomic resolution of the studied plant organs (Akhmetiev 2004). The evolution of continental Paleogene climates has been well studied on the basis of palaeobotanical data from Australia, Europe and North America (Greenwood and Wing 1995; Wilf 2000; Wing and Harrington 2001; Jolley and Widdowson 2005; Mosbrugger et al. 2005; Wing et al. 2005; Utescher et al. 2007; Greenwood et al. 2010; Utescher et al. 2011) and marine proxy data from both hemispheres (Pearson et al. 2007; Zachos et al. 2008; Bijl et al. 2009). In East Asia, quantitative Paleogene climatic reconstructions on the basis of palaeobotanical data have been conducted on individual sites of China (e.g. He and Tao 1997; Quan and Zhang 2005; Su et al. 2009; Hao et al. 2010; Wang et al. 2010; Hoorn et al. 2012; Quan et al. 2012).

As regards the Paleogene climate evolution in the RFE in general and Primorye, in particular, our knowledge is still very poor and fragmentary. Using the Climate Leaf Analysis Multivariate Program (CLAMP), Paleogene climatic reconstructions have been made by Budantsev (1997, 1999) for the northeastern part of the RFE, mostly for western Kamchatka. Based on an example of the Irgirninskaya flora of western Kamchatka, Budantsev (1997, 1999) obtained quantitative characteristics of the late Eocene palaeoclimate. The reconstructed conditions were compared to those of the modern climate of the Atlantic states of the USA, between 41–43° N and 73–75° W, characterised by cool summers and mild winters, and a uniform distribution of abundant rainfall typical of the temperate zone (Budantsev 1997, 1999). For the northeastern part of the RFE, Popova et al. (2012), using the Coexistence Approach (CA), document the transition from very warm and humid conditions in the late Oligocene via the Middle Miocene Climatic Optimum to a cool temperate climate during the Pliocene. For the southern part of Primorye, a first quantitative climate record was presented by Utescher et al. (2015) based on 14 floras and covering the time span from the middle Eocene to early Pleistocene.

In the present detailed study, we use the exceptionally rich palaeobotanical heritage of Primorye to reconstruct the Paleogene regional climate evolution in space and time, and to trace potentially monsoon-induced patterns. Based on a total of 54 reasonably well-dated pollen and leaf floras from 19 basins, coherent climate maps are presented for the first time for seven stratigraphic levels covering climate evolution in a time span of ca. 42 myr, in total. All the climate data are reconstructed using a single approach applicable on every plant organ type (Coexistence Approach—CA).

Study area and palaeogeographical settings

Study area

The palaeobotanical records of Primorye studied herein originate from 19 basins (Fig. 1). The Paleogene strata of Primorye

Fig. 1 Map showing the location of the Primorye Region within the Russian Far East (**a**) and map over Primorye showing the location of the studied basins (**b**). Dotted line: contours of the basins after Pavlyutkin and Petrenko (2010). 1, Khasanskii (Kraskino9182/9196 and Gladkaya17 floras); 2, Ambinskii (Zanadvorovka flora); 3, Artemo-Tavrichanskii (Tavrichanka9142, Vol'no-Nadezhdinskoe and Bolotnaya floras); 4, Shkotovskii (Shkotovo and Smolyaninovo floras); 5, Pushkinskii (Pushkinskii9180 and Terekhovka floras); 6, Vanchinskii (Kluch Ugolnyi flora); 7, Ivanovskii (Ivanovka610 flora); 8, Pavlovskii (Pavlovka9035-D flora); 9, Snegurovskii (Rettikhovka flora); 10, Chernyshevskii (Arsen'evka flora); 11, Zerkal'nenskii (Voznovo9206, Svetlyi, Kluch Tuyanov and Ustinovka floras); 12, Tur'erogskii (Turii Rog8 flora); 13, Krylovskii (Krylovskii524 flora); 14, Kemskii (Tikhii Kluch flora); 15, Nizhnebikinskii (Luchegorsk6212, Luchegorsk and Luchegorsk540/541 floras); 16, Amginskii (Amgu9302 flora); 17, Maksimovskii (Kluch Stolbikova, Kluch Kedrovyi and Sobolevka floras); 18, Svetlovodnenskii (Salibeza flora); 19, Ozero Toni (Ozero Toni flora). The single floras are listed in Table 1, together with information on basin provenience, type of flora, stratigraphic age, method of dating and references. The complete floral lists, assigned NLRs and their climatic requirements are given in the Electronic Supplement 1

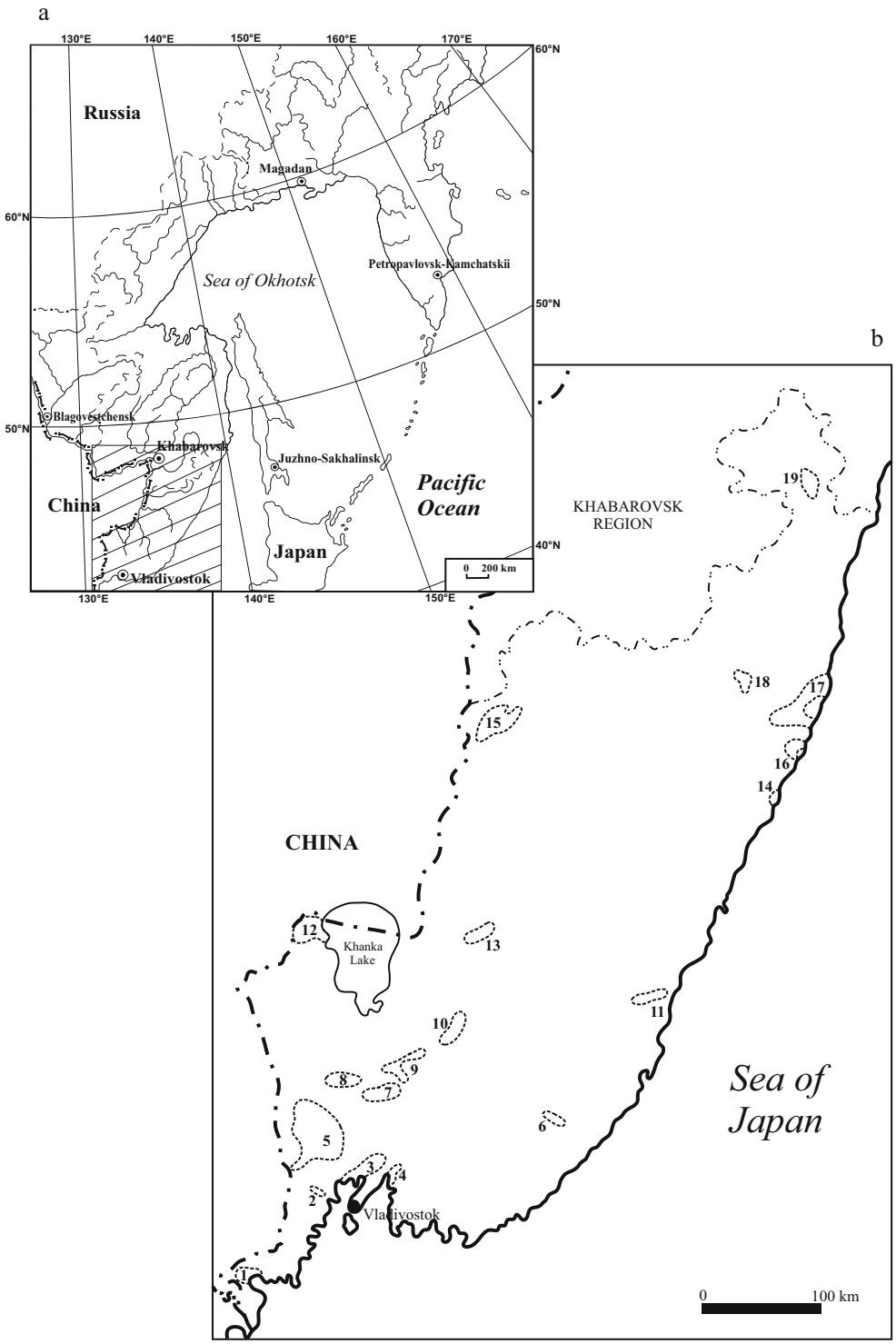

comprise volcanic and sedimentary deposits, unconformably overlying Mesozoic basement. The sedimentary facies includes fine- to coarse-grained continental clastics and intercalated lignites excavated in several active opencast mines. For some basins, mainly generated by extensional tectonics (Pavlovskii, Pushkinskii and Maksimovskii Basins), intercalated volcanoclastic layers and tholeitic lava flows (Maksimovskii Basin: Takhobinskaya and Kuznetsovskaya formations) allow for radiometric dating of the strata (Table 1; Fig. 2). The sedimentary successions in the individual basins are characterised by numerous unconformities related to regional tectonics and phases of rifting and subsidence (Pavlyutkin and Petrenko 2010). When combining the strata of the individual basins, a time span of

Table 1 Palaeofloras studied. P, palynofloras; L, leaf flora; IRC, inter-regional correlation based on palaeobotany

Stratigraphic level	Locality name	Lon	Lat	Type of flora	Fossil taxa/taxa with climate data	Basin, formation	Age, method of dating	References
1. Late Oligocene	1. Zanadvorovka	131.40	43.20	P	30/28	Ambinskii, analog of Pavlovskaya	Chattian, K/Ar dating (24.0 ± 3.0 Ma), IRC	Pavlyutkin and Petrenko 2010; Popov et al. 2007
	2. Pushkinskii9180	131.50	43.30	P L	30/28 28/26	Pushkinskii, Pavlovskaya	Chattian, IRC	Pavlyutkin et al. 2012
	3. Pavlovka9035-D	132.05	44.05	P	35/32	Pavlovskii, Pavlovskaya	Chattian, IRC	Pavlyutkin and Petrenko 2010
	4. Turii Rog8	131.60	45.10	P	32/30	Tur'erogskii, analog of Pavlovskaya	Chattian, IRC	Pavlyutkin and Petrenko 2010
	5. Luchegorsk6212	134.20	46.30	P	32/30	Nizhnebikinskii, Upper Coal	Chattian, IRC	Pavlyutkin and Petrenko 2010
2. Early Oligocene	6. Kraskino9182/9196	130.40	42.45	P L	71/63 161/148	Khasanskii, Nizhnefatashinskaya	Rupelian, IRC	Pavlyutkin et al. 2014
	7. Pavlovka9035-D	132.05	44.05	P	37/34	Pavlovskii, Pavlovskaya	Rupelian, IRC	Pavlyutkin and Petrenko 2010
	8. Rettikhovka	132.40	44.10	P L	36/33 48/43	Snegurovskii, analog of Pavlovskaya	Rupelian, IRC	Ablaev 1977; Akhmetiev et al. 1973; Klimova et al. 1977; Pavlyutkin and Petrenko 1994, 2010
	9. Voznovo9206	135.30	44.15	P L	79/67 80/67	Zerkal'nenskii, Voznovskaya	Rupelian, IRC	Pavlyutkin et al. 2014
	10. Tikhii Kluch	137.10	45.40	L	49/39	Kemskii, Kizinskaya	Rupelian, IRC	Akhmetiev 1988; Rybalko et al. 1980; Varnavskii et al. 1988
	11. Amgu9302	137.36	45.60	L	62/57	Amginskii, Granatnenskaya	Rupelian, IRC	Akhmetiev 1988; Akhmetiev and Shyvareva 1989; Klimova 1981, 1988; Pavlyutkin et al. 2014
	12. Maksimovka	137.50	46.05	L	81/71	Maksimovskii, Maksimovskaya	Rupelian, IRC	Akhmetiev 1988; Rybalko et al. 1980; Varnavskii et al. 1988
3. Late Eocene	13. Gladkaya17	130.50	42.40	P L	41/36 33/28	Khasanskii, Khasanskaya (= Nazimovskaya)	Priabonian, K/Ar dating (35.6–36.0 Ma), IRC	Chashchin et al. 2013; Gromova 1980; Pavlyutkin and Petrenko 1997, 2010; Pavlyutkin et al. 2006, 2014
	14. Tavrichanka9142	131.50	43.20	P L	46/40 75/70	Artemo-Tavrichanskii, Ust'-davydovskaya	Priabonian, vertebrate fauna, IRC	Flerov et al. 1974; Pavlyutkin 2007; Pavlyutkin and Petrenko 1993, 2010; Pavlyutkin et al. 2006; Yanovskaya 1954
	15. Shkotovo	132.15	43.20	P	26/22	Shkotovskii, Upper Coal Fm.	Priabonian, IRC	Pavlyutkin and Petrenko 2010
	16. Ivanovka610	132.30	43.60	P	50/44	Ivanovskii, analog of Pavlovskaya	Priabonian, IRC	Pavlyutkin and Petrenko 2010
	17. Pavlovka9035-D	132.05	44.05	P L	50/43 25/21	Pavlovskii, Pavlovskaya	Priabonian, IRC	Bolotnikova 1993, 1994; Pavlyutkin and Petrenko 2010; Varnavskii et al. 1988
	18. Svetlyi	135.10	44.10	P L	14/13 22/16	Zerkal'nenskii, Svetlinskaya	Priabonian, IRC	Mikhailov et al. 1989; Pavlyutkin and Petrenko 2010
	19. Luchegorsk	134.20	46.30	P L	61/48 56/47	Nizhnebikinskii, Bikinskaya	Priabonian, IRC	Ablaev et al. 2006; Bolotnikova and Sedykh 1987; Koshman 1964; Kundyshev and Verkhovskaya 1989
	20. Salibeza	137.50	46.05	L	48/38	Svetlovodnenskii, Salibezskaya	Priabonian, IRC	Klimova and Tsar'ko 1989; Varnavskii et al. 1988
4. Middle Eocene	21. Vol'no-Nadezhdinskoe	131.50	43.20	P L	59/49 25/20	Artemo-Tavrichanskii, Nadezhdinskaya	Bartonian, IRC	Akhmetiev et al. 1978; Pavlyutkin 2007; Pavlyutkin and Petrenko 1993, 2010
	22. Bolotnaya	131.05	43.20	P	45/41		Lutetian, IRC	

Table 1 (continued)

Stratigraphic level	Locality name	Lon	Lat	Type of flora	Fossil taxa/taxa with climate data	Basin, formation	Age, method of dating	References
				L	75/70	Artemo-Tavrichanskii, Nadezhdinskaya		Ablaev 2000; Ablaev and Akhmetiev 1977; Akhmetiev 1973; Kundyshev and Petrenko 1987; Pavlyutkin 2007; Pavlyutkin and Petrenko 2010
	23. Shkotovo	132.15	43.20	P	31/27	Shkotovskii, Nadezhdinskaya	Middle Eocene, IRC	Baskakova and Gromova 1982
	24. Terekhovka	131.30	43.40	P	44/39	Pushkinskii, Nadezhdinskaya	Middle Eocene, IRC	Pavlyutkin and Petrenko 2010
	25. Luchegorsk540/541	134.20	46.30	P	33/29	Nizhnebikinskii, Luchegorskaya	Middle Eocene, IRC	Pavlyutkin and Petrenko 2010
5. Early Eocene	26. Tavrichanka9142	131.50	43.20	P	58/48	Artemo-Tavrichanskii, Uglovskaya	Ypresian, IRC	Pavlyutkin and Petrenko 2010
	27. Smolyaninovo	132.30	43.20	P	56/48	Shkotovskii, Uglovskaya	Ypresian, IRC	Baskakova and Gromova 1979, 1984; Pavlyutkin and Petrenko 2010; Tashchi et al. 1996; Varnavskii et al. 1988; Verkhovskaya and Kundyshev 1989
				L	42/39			
	28. Kluch Ugolnyi	134.10	43.30	P	19/16	Vanchinskii, analog of Uglovskaya	Ypresian, IRC	Chekryzhov et al. 2010; Pavlyutkin and Petrenko 2010
				L	20/15			
	29. Rettikhovka	132.40	44.10	P	56/46	Snegurovskii, analog of Uglovskaya	Ypresian, IRC	Pavlyutkin and Petrenko 2010
	30. Arsen'evka	133.10	44.10	P	57/44	Chernyshevskii, analog of Uglovskaya	Ypresian, IRC	Bolotnikova 1988
	31. Kluch Tuyanov	135.10	44.10	L	62/52	Zerkal'nenskii, Tuyanovskaya	Ypresian, IRC	Baskakova and Lepekhina 1990; Varnavskii et al. 1988
	32. Krylovskii524	133.40	45.10	P	59/51	Krylovskii, Uglovskaya	Ypresian, IRC	Pavlyutkin and Petrenko 2010
	33. Luchegorsk540/541	134.20	46.30	P	58/45	Nizhnebikinskii, Lower Coal Fm.	Ypresian, IRC	Pavlyutkin and Petrenko 2010
				L	12/9			
	34. Ozero Toni	138.30	47.40	P	32/30	Ozero Toni, Kizinskaya	Early Eocene, IRC	Oleinikov and Klimova 1977; Varnavskii et al. 1988
				L	44/36			
6. Late Paleocene	35. Ustinovka	135.10	44.10	L	25/22	Zerkal'nenskii, Tadushinskaya	Selandian, IRC	Pavlyutkin and Petrenko 2010
	36. Kluch Stolbikova	137.50	46.05	L	14/10	Maksimovskii, Kuznetsovskaya	Thanetian, K/Ar dating (55.0 Ma), IRC	Pavlyutkin and Petrenko 2010; Varnavskii et al. 1988
	37. Kluch Kedrovyi	137.78	46.17	P	37/34	Maksimovskii, Kedrovskaya	Thanetian, IRC	Varnavskii et al. 1988
7. Early Paleocene	38. Ustinovka	135.10	44.10	L	31/26	Zerkal'nenskii, Bogopol'skaya	Danian, IRC	Ablaev et al. 2005; Krassilov 1989
	39. Sobolevka	137.50	46.05	L	64/56	Maksimovskii, Takhobinskaya	Danian, K/Ar dating (64.0 Ma), IRC	Akhmetiev 1973, 1988; Borsuk 1952

References and complete flora lists including Nearest Living Relatives used for climate calculations are given in Online Resource 1

ca. 42 myr is represented, spanning the early Paleocene (Danian) to late Oligocene (Chattian).

The regional stratigraphic correlation chart for the basins (Fig. 2; adapted from Pavlyutkin and Petrenko 2010) is based on a variety of stratigraphic data obtained from radiometric dating, regional and inter-regional pollen zonation, as well as lithological, palaeobotanical and vertebrate fauna correlations (Akhmetiev 1973; Varnavskii et al. 1988; Popov et al. 2005; Pavlyutkin and Petrenko 2010; Chashchin et al. 2013). The stratigraphic scheme has been tied to the International Stratigraphic Chart (Pavlyutkin and Petrenko 2010; Cohen et al. 2013) and allows for dating the flora-bearing horizons at the stage level (Fig. 2). For some of the floras, stratigraphic ages are better constrained (cf. Table 1: radiometric datings for the Zanadvorovka, Gladkaya17, Kluch Stolbikova and Sobolevka floras).

Palaeogeographical setting

The geological situation of Primorye and the adjacent territory of northeastern China constitute a single continental area since the late Cretaceous, together with the inner zone of Japan and Korea, prior to the opening of the Sea of Japan (Maruyama et al. 1997). This opening, caused by intracontinental rifting, set on to the south of our study area. The initial rifting stage took place in the middle Eocene, while the major phase

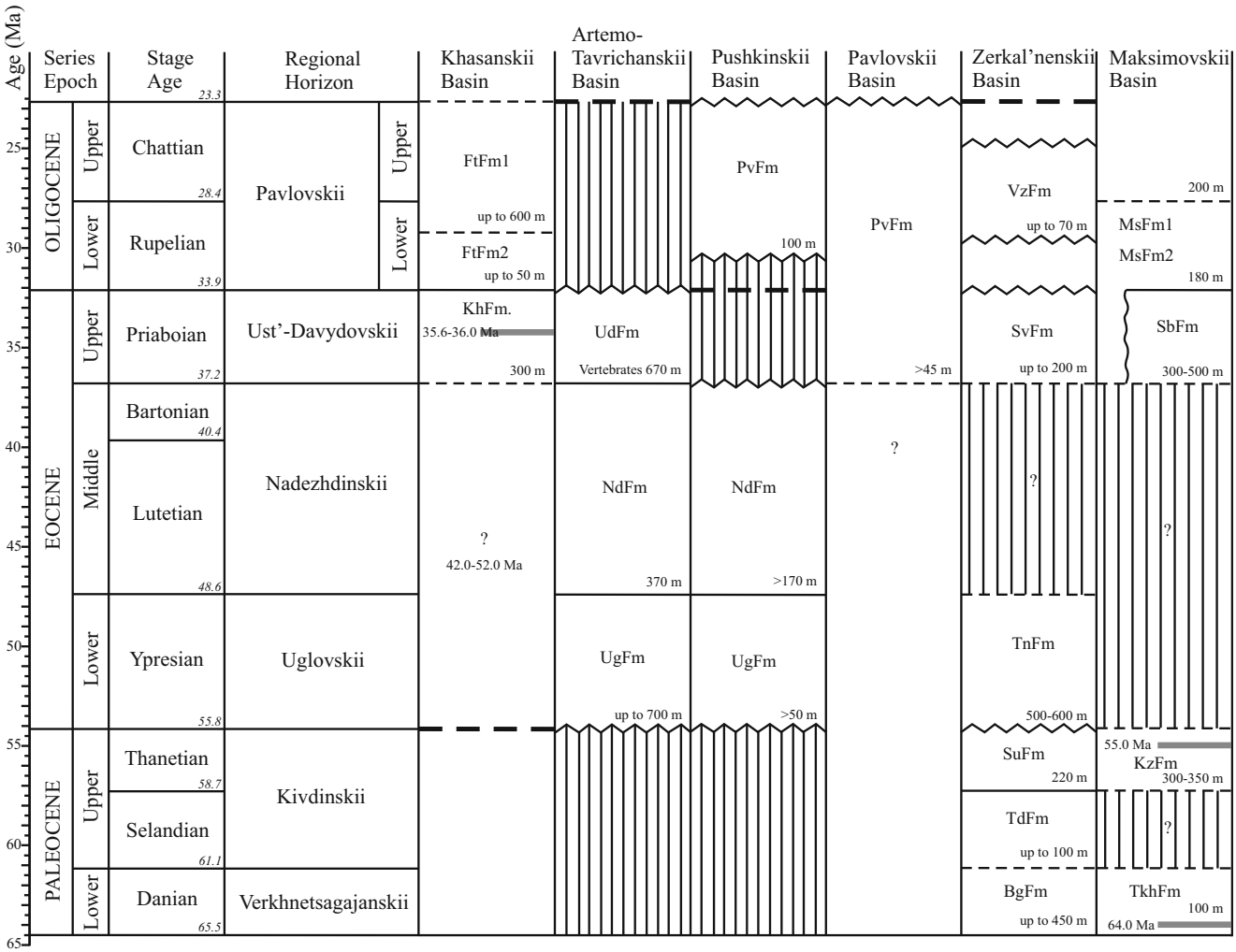

Fig. 2 Regional stratigraphic chart for the Paleogene sediments of some Cenozoic basins of Primorye considered in this study (modified from Pavlyutkin and Petrenko 2010), tied to the international standard (Cohen et al. 2013). Jagged boundary: unconformably overlying. Vertical stipple: gap in sedimentation. Details on the palaeofloras are given in Table 1. BgFm, Bogopol'skaya Formation; TkhFm, Takhobinskaya Formation (radiometric age 64.0 Ma by Akhmetiev 1973); TdFm, Tadushinskaya Formation; SuFm, Suvorovskaya Formation; KzFm, Kuznetsovskaya Formation (radiometric age 55.0 Ma by Varnavskii et al. 1988); UgFm, Uglovskaya Formation; TnFm, Tuyanovskaya Formation; NdFm, Nadezhdinskaya Formation; KhFm, Khasanskaya Formation; UdFm, Ust'-davydovskaya Formation (radiometric age 35.6–36.0 Ma by Chashchin et al. 2013); SvFm, Svetlinskaya Formation; SbFm, Salibezskaya Formation; FtFm, Fatashinskaya Formation; PvFm, Pavlovskaya Formation; VzFm, Voznovskaya Formation; MsFm, Maksimovskaya Formation

occurred considerably later, during the early to middle Miocene (Denisov 1965; Golozubov 2006). These geological settings fully confirm the conclusion drawn from palaeobotany, regarding the commonality in the Mesozoic and earlier Paleogene phyto-history of this region (Kawai et al. 1962; Pavlyutkin and Golozubov 2010). When taking into account these considerations, we have to assume that the Paleogene geography fundamentally differed from modern conditions. Unlike today, the Pacific coast was located several hundred kilometres to the east of our study area, throughout the time span regarded, and thus a direct maritime impact on the regional palaeoclimate probably did not exist (Fig. 3). To illustrate the palaeogeographical configuration of Primorye in the middle Eocene (ca. 45 Ma), we used the OSDN plate reconstruction (hotspot reference frame) and palaeogeographic reconstructions by Maruyama et al. (1997) and Pavlyutkin and Golozubov (2010).

The Cenozoic sedimentary basins of southern Primorye such as the Khasanskii, Shkotovskii and Zerkal'nenskii Basins are related to rifting and extensional tectonics. The subsidence of the basins was accompanied by volcanic activities. Though block tectonics may have caused minor level differences, a near sea-level elevation can be assumed for the palaeofloras recovered from these basins (Lebedeva 1957; Denisov 1965; Khudyakov et al. 1972).

The Sikhote-Alin Range, located in the northeast of Primorye, represents a continental-margin range including late Cretaceous to Paleogene volcanites and intrusives (Parfenov et al. 2009). There is evidence for intensified uplift of this mountain range from the Eocene–Oligocene transition on. At the same time, older depressions subsided as intramontane basins, namely the Artemo-Tavrichanskii and Vanchinskii Basins in the southwest of Primorye. It is largely unclear which elevation the Sikhote-Alin had attained in Paleogene times. However, palaeofloras reconstructed on the basis of fossil plant remains from the several Paleocene volcanic complexes allowed the suggestion that, within northeast Primorye, the elevation of the Sikhote-Alin exceeded 500 m a.s.l. (Akhmetiev et al. 2009). From the second half of the Eocene to Miocene, there was an intensive uplift of this ridge (Parfenov et al. 2009). Oleinikov and Oleinikov (2005) estimate the elevation of the Sikhote-Alin Mountains in the central part of Primorye in the late Miocene equal to 700–800 m a.s.l. The most recent uplift pulse of the Sikhote-Alin, however, occurred in the Pliocene and Quaternary, connected to basaltic eruptions. The elevation, which attains 1000–1400 m a.s.l at the watershed of the Sikhote-Alin Mountains, created a modern mountainous relief with heights of up to 1856 m a.s.l. and co-occurred with increased subsidence in the neighbouring part of the Sea of Japan and the Tatar Strait (Kropotkin and Shakhvarstova 1965).

According to the available palaeomagnetic data, the eastern part of Eurasia occupied a position close to the modern one, i.e. did not experience any significant displacements or rotations since the Late Jurassic (Lee et al. 1987; Zhu 1993; Ushimura et al. 1996; Kolesov 2003). At the same time, palaeomagnetic data for the pre-Cenozoic formations of Japan indicate that these rocks were formed much to the south of their present location (Hirooka 1990). This is attributed to interactions with the relatively immobile Eurasia and the extremely mobile oceanic plate of Isanagi (Golozubov 2006). According to Utescher et al. (2015), as regards plate tectonic movement, a southward displacement of Primorye by ca. 2° latitude occurred since the middle Eocene (Ocean Drilling Stratigraphic Network, GEOMAR plate reconstruction service using hotspot reference frame), thus decreasing the measured cooling signal.

Materials and methods

The floral record

The palaeobotanical record of Primorye is diverse and has been the subject to extensive taxonomic studies (cf. Table 1 for references). In this study, all palaeofloras considered here were carefully re-evaluated regarding the validity of taxonomic identifications and the Nearest Living Relatives (NLRs) of the fossil taxa, i.e. the taxonomical concept of the fossil materials and modern botanical affinity were carefully revised. In the present study, a total of 54 floras including 30 palynofloras (PF) and 24 leaf floras (LF) were studied with respect to palaeoclimate at seven stratigraphic levels. The floras cover a total time span of ca. 42 myr, ranging from the early Paleocene (Danian) to late Oligocene (Chattian). The single floras are listed in Table 1, together with information on basin provenience, type of flora, stratigraphic age, method of dating and references. The complete floral lists, assigned NLRs and their climatic requirements are given in the Online Resource 1.

Quantitative palaeoclimate reconstruction—application of the Coexistence Approach

To reconstruct climate from the plant fossil record of Primorye, we use the Coexistence Approach (CA) (Mosbrugger and Utescher 1997; Utescher et al. 2014). This approach is organ-independent, so that both macro- and microfossil plants are eligible as long as their modern botanical affinities are determinable (Mosbrugger and Utescher 1997; Utescher et al. 2007; Bruch et al. 2011). For a detailed description of the method, the reader is referred to the original papers describing the procedure (Mosbrugger and Utescher 1997; Utescher et al. 2014). We use data sets from the Palaeoflora Database (Utescher and Mosbrugger 2018) together with ca. 40 newly compiled records as source for climatic requirements of extant plant taxa. All modern data are made available

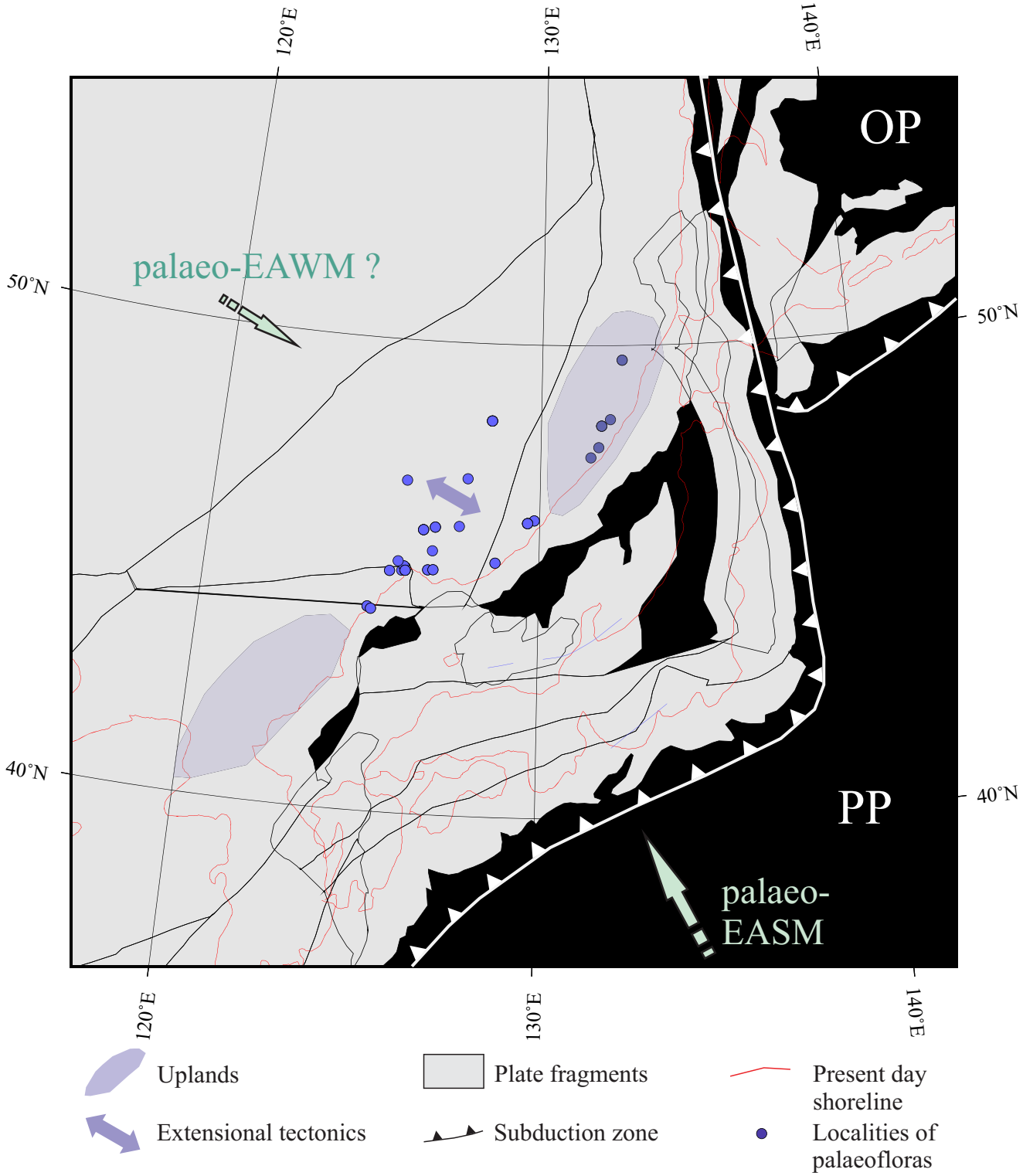

Fig. 3 Palaeogeographic reconstruction of Primorye for 45 Ma. Basemap: OSDN plate reconstruction using the hotspot reference frame (www.odsn.de), additional palaeogeographic and tectonic information from Maruyama et al. (1997) and Pavlyutkin and Golozubov (2010), with supposed atmosheric circulation systems. PP, Pacific Plate; OP, Okhotsk Plate; EASM, East Asian Summer Monsoon; EAWM, East Asian Winter Monsoon

in Online Resource 2. The new records were compiled using chorological information from Fang et al. (2009, 2011) and Sokolov et al. (1977, 1980, 1986) and climatological datasets from Müller and Hennings (2000) and New et al. (2002).

Climate data entries already available in the database were carefully checked for completeness. Floral lists with corresponding NLRs employed in this study and their climatic requirements are made available in the Online Resource 1.

In this study, three temperature and four precipitation variables are reconstructed: mean annual temperature (MAT), cold and warm month mean temperature (CMMT, WMMT), mean annual precipitation (MAP) and mean monthly precipitation of the wettest, driest and warmest month (MPwet, MPdry and MPwarm). In the CA, at least 10 NLR taxa contributing with climate data are required to obtain reliable results (Mosbrugger and Utescher 1997). Here, 9 to 148 taxa contribute to determining the climate data (Table 1). Except for the early Eocene Luchegorsk540/541 flora (LF 33) with only nine taxa, the palaeofloras are diverse enough to obtain reliable results. The climatic resolution of the CA results also depends on the taxonomical level of NLR identification (Mosbrugger and Utescher 1997). *Sciadopitys verticillata* and *Comptonia peregrina* were excluded from the analysis for being permanent climatic outliers in other CA-based climate reconstructions from Cenozoic palaeofloras of the mid-latitudes (Utescher et al. 2014), likewise *Parrotia persica* and *Cercidiphyllum japonicum* because of their present endemic or relict status (Utescher et al. 2015). Moreover, 40 (sub)-cosmopolitan taxa were not considered in CA analysis, for a total of 14 taxa climatic tolerances could not reliably be identified (cf. Online Resource 2). *Alchonea*, Bombacaceae, Brownlowioideae, *Brucea, Cedrela* and *Kleinhovia*, distributed in the subtropical to tropical realm, were identified as warm outliers in the analysis while *Larix* represents a cold outlier. *Larix* is mainly present in pollen records and interpreted as an altitudinal element. To avoid interference in precipitation reconstruction, the taxon was excluded from the CA calculations. Its occurrence is discussed separately (see Disscusion).

To illustrate climate change in Primorye during the Paleogene, the floras are allocated to seven time intervals. Time intervals are defined according to the international standard: early and late Paleocene, early, middle and late Eocene and early and late Oligocene. To visualise the results, a series of maps is provided and discussed below (cf. Figs. 4, 5 and 6). These maps show the evolution of the six climate variables analysed in seven Paleogene stages regarded and are based on means of coexistence intervals for each palaeoflora (Table 2) and averaged for the time intervals regarded (Table 3). The complete set of coexistence intervals for all floras and climate variables studied is provided in Online Resource 3. For the technical preparation of the maps, ArcMAP 10.4 was used. To graphically depict the temporal climate evolution of Primorye, we use box-and-whisker diagrams based on variable means from Table 2, grouped by time slice (box plots, PAST software; Figs. 7 and 8). The box plots for MATmean are shown next to the benthic oxygen isotope record after Zachos et al. (2008) (Fig. 7a, b).

Climate seasonality, monsoon intensity

In order to determine temperature seasonality of the Paleogene climate of Primorye, the mean annual range of temperature (MART) was calculated as the difference of WMMT and CMMT for the time intervals studied (Table 3). To study precipitation seasonality, the mean annual range of precipitation (MARP—calculated as difference of MPwet and MPdry) was calculated for the time intervals (Table 3). In order to measure the EAM intensity during the Paleogene, we use the ratio of MPwet and MPdry on MAP (RMPwet and RMPdry) (Table 3). According to Jacques et al. (2011), the ratios of MPwet and MPdry of MAP are good indication of past monsoon intensity (summer—EASM and winter—EAWM, respectively). The monsoon is a complex climatic phenomenon; nevertheless, in general, the increasing of RMPwet, i.e. higher proportion of precipitation in the wet season, may indicate the intensification of EASM, while the decreasing of RMPdry, i.e. lower proportion of precipitation in the dry season, suggests the intensification of EAWM. To visualise the results, change of the MART and MARP, the RMPwet and RMPdry are taken as a measure of monsoon intensity and are shown as box plots in Fig. 9.

Results

Complete lists of taxa for each of the localities, including their NLRs with climatic requirements, are provided in the Online Resource 1. Climate data calculated for the 54 floras are given in the Online Resource 3.

To analyse the climate change of Primorye during the Paleogene in space and time, palaeoclimate data presently reconstructed for six different climate variables (MAT, CMMT, WMMT, MAP, MPwet and MPdry) are shown in the map series for seven time intervals in comparison with modern conditions. Gradients and patterns obtained for single climate variables are shown in Figs. 4, 5 and 6. Means of seven climate variables for each time interval and variables of climate seasonality and monsoon indices calculated from these means are given in Tables 2 and 3, and illustrated in Figs. 7, 8 and 9. Changing climate patterns can continuously be studied for the time span from the early Paleocene to late Oligocene. The given figures in each case refer to means and CA intervals (Xmean (Xmin–Xmax)).

Temperature

The mean values of MAT indicate a general cooling trend from ca. 17.5 °C in the late Paleocene and early to middle

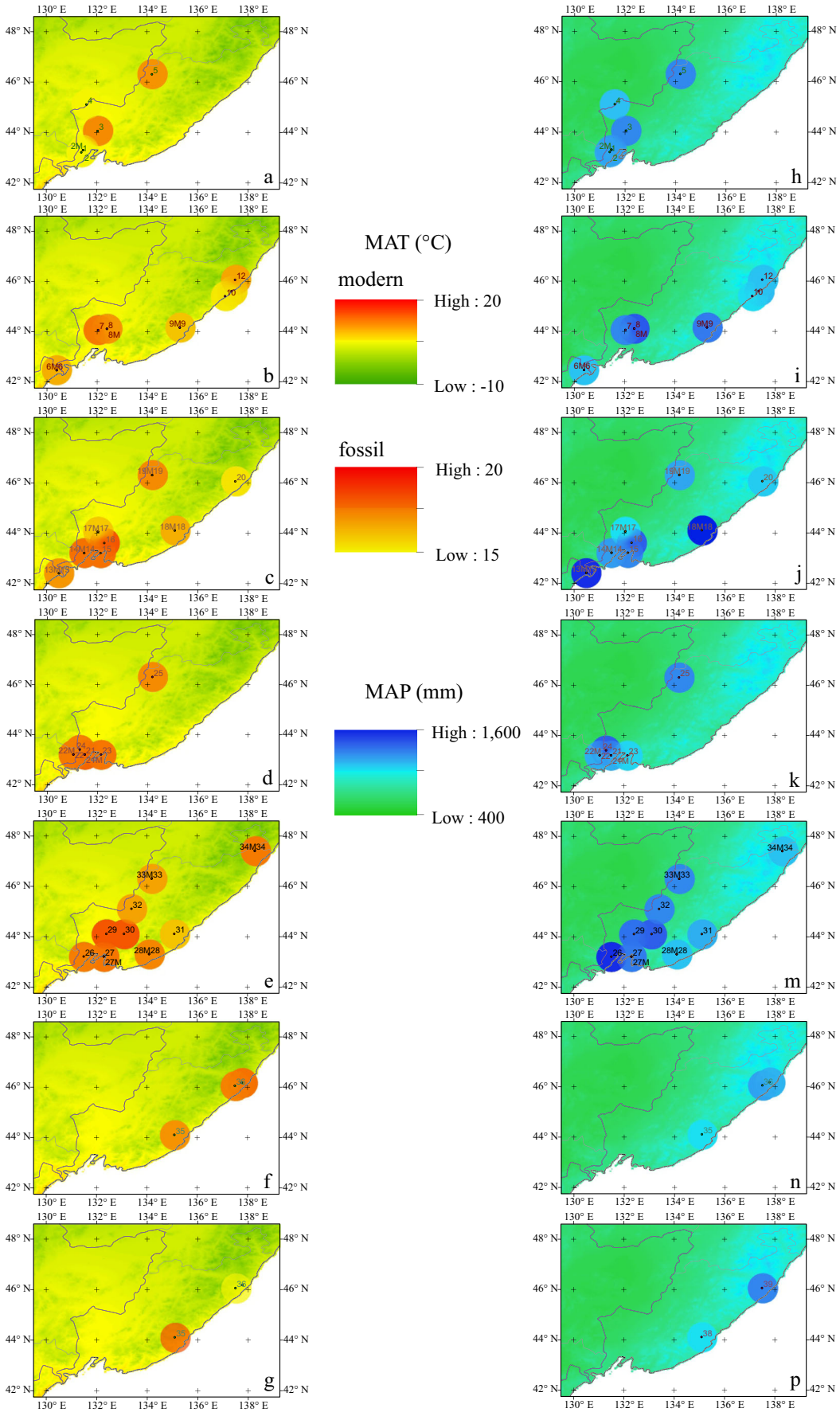

◀ **Fig. 4** MAT (**a**–**g**) and MAP (**h**–**p**) in the Paleogene of Primorye in comparison with modern. **a**, **h** Late Oligocene. **b**, **i** Early Oligocene. **c**, **j** Late Eocene. **d**, **k** Middle Eocene. **e**, **m** Early Eocene. **f**, **n** Late Paleocene. **g**, **p** Early Paleocene. Maps are generated using ArcMAP 10.4. Modern climate data: WorldClim–Global Climate Data (www.worldclim.org). Small black discs with numbers refer to fossil sites in Table 1. Palaeoclimate data (coloured discs): interpolated means of coexistence intervals using Spatial Analyst (IDW method, power 2, and fixed search radius)

Eocene to ca. 16 °C in the early Oligocene, with a warm pick in the middle Eocene (Table 3, Fig. 7a). The Paleocene is represented by few sites in the coastal area (Table 2, Fig. 4f, g). The highest MAT values are indicated for the early Paleocene LF 38 (central part)—18.4 °C (16–20.8 °C), while for the other floras of both Paleocene time slices cooler CA intervals are obtained (early Paleocene LF 39 (northeast)—14.5 °C (13.4–15.6 °C); late Paleocene PF 37 (northeast)—17.6 °C (13.8–21.4 °C), LF 35 (central part)—16.9 °C (12.8–21.1 °C)). In the Eocene (Table 2, Fig. 4c–e), the warmest MAT intervals are indicated for the early Eocene PF 27, 28, 29 and 30 (southwest and central part)—18.2 °C (15.3–21.1 °C), for the middle Eocene LF 22 (the southernmost flora)—18 °C (16.7–19.4 °C) and for the late Eocene PF 16 (southwest)—18.2 °C (15.3–21.1 °C). The lowest MAT values are reconstructed for the early Eocene LF 34, the northeasternmost coastal flora of our record (15.1 °C (13.8–16.5 °C)). In the Oligocene (Table 3, Fig. 4a, b), lower boundaries of MAT intervals all are below 15 °C. More specific MAT intervals (early Oligocene LF 8 (southwest)—14.8 °C (14–15.6 °C); late Oligocene LF 2 (southwest)—14.4 °C (13.3–15.5 °C)) are obtained from floras in the southwest of the study area.

For the CMMT means indicate a high level of ca. 7–10 °C persisting throughout the Paleocene and Eocene followed by a pronounced cooling trend towards the Oligocene where CMMT means at ca. 4.5–6.5 °C (Table 3, Fig. 7c). The highest values of CMMT in the Paleocene (Table 2, Fig. 5f, g) are indicated for the early Paleocene LF 38 (central part)—9.7 °C (9–10.4 °C), the other sites provided wider CMMT intervals with values > ca. 6 °C (PF 37 (northeast)—10 °C (6.1–13.9 °C); LF 39 (northeast)—8.5 °C (6.6–10.4 °C)). The coolest Paleocene CMMT is obtained for LF 35 (central part)—3.8 °C (− 2.8 to 10.4 °C). In the Eocene (Table 2, Fig. 5c–e), the warmer CMMT intervals range from ca. 6–12 °C (early Eocene PF 27 (southwest)—9.6 °C (6.6–12.6 °C), middle Eocene PF 22 (the southernmost flora)—9.7 °C (7.7–11.8 °C)). Significantly cooler conditions with CMMT in the order of 0–5 °C are indicated for two leaf floras from the northeast and central part (early Eocene LF 34—3.9 °C (3.1–4.8 °C); late Eocene LF 18—2.2 °C (− 0.1 to 4.6 °C)). For the Oligocene (Table 3, Fig. 5a, b), the highest CMMT values are obtained for the early Oligocene PF 7 (southwest)—8.2 °C (3.8–12.6 °C), while data from leaf floras did not exceed 5 °C (early Oligocene LF 9 (northeast)—4.3 °C (3.5–5.1 °C); late Oligocene LF 2 (southwest)—2.2 °C (− 0.1 to 4.5 °C)).

WMMT means indicate lower values for the early Paleocene, a high level of ca. 25.5–26.5 °C from the late Paleocene to early Oligocene, and again cooler conditions during the late Oligocene (Table 3, Fig. 7d). Typical WMMT values reconstructed for the Paleocene (Table 2, Fig. 5n, p) are ca. 25–26.5 °C (early Paleocene LF 39 (northeast)—25.1 °C (24–26.3 °C); late Paleocene PF 37 (northeast)—26.5 °C (24.7–28.3 °C)). Sligtly higher WMMTs are indicated for the Eocene (Table 2, Fig. 5j, k, m), mainly for the southwest of the study area with 26.6–28.1 °C (early Eocene PF 26; middle Eocene PF 21; late Eocene PF 13 and 14 (all southwest)). Lower values result for the early Eocene LF 33 (central part)—24.2 °C (19.6–28.8 °C), for the middle Eocene PF 22 (the southernmost flora)—25.2 °C (23.6–26.8 °C) and for the late Eocene LF 18 (central part)—24.6 °C (22.5–26.8 °C). Most of the early Oligocene WMMT values (Table 3, Fig. 5h, i) are still at a high level (e.g. early Oligocene PF 6—27.4 °C (26.6–28.2 °C); late Oligocene LF 2 (southwest)—26.1 °C (24.7–27.5 °C)). In several late Oligocene floras, the lower WMMT limit of CA intervals declines to ca. 20 °C (PF 1, 2 and 4—24 °C (20.2–27.8 °C)).

Precipitation

MAP shows a general increase from ca. 1050–1200 mm in the late Paleocene to ca. 1150–1400 mm recorded throughout the Eocene, followed by a minor decline in the Oligocene (Table 3, Fig. 8a). The highest Paleocene values of MAP (Table 2, Fig. 4n, p) are indicated for the northeast of the study area (early Paleocene LF 39—1293 mm (1231–1355 mm)); the lowest values are obtained for sites in the central part (early Paleocene LF 38—1045 mm (735–1355 mm); late Paleocene LF 35—1045 mm (735–1355 mm)). For the Eocene (Table 2, Fig. 4j, k, m), very high MAP of over 1500 mm is obtained for the middle Eocene PF 21 (southwest—1554 mm (1531–1577 mm)), while sites in the east and northeast tend to lower values (early Eocene LF 34 (northeast)—1047 mm (740–1355 mm)). In the Oligocene (Table 3, Fig. 4h, i), the highest values again result for the southwest (early Oligocene PF 8—1422 mm (1231–1613 mm)), other sites indicate a MAP of at least 900 mm for the early Oligocene, and possibly drier conditions with MAP > ca. 650 mm for the late Oligocene (PF 4 (central part)—1132 mm (652–1613 mm)).

MPwet steadily increased from ca. 175 mm in the early Paleocene to the middle Eocene (median value at 215 mm), and then decreased again towards the early Oligocene. The late Oligocene MPwet was again at a higher level (Table 3, Fig. 8b). The highest values of MPwet in the Paleocene (Table 2, Fig. 6f, g) are indicated for the early Paleocene LF 38 (central part)—181 mm (167–195 mm); MPwet ranges of

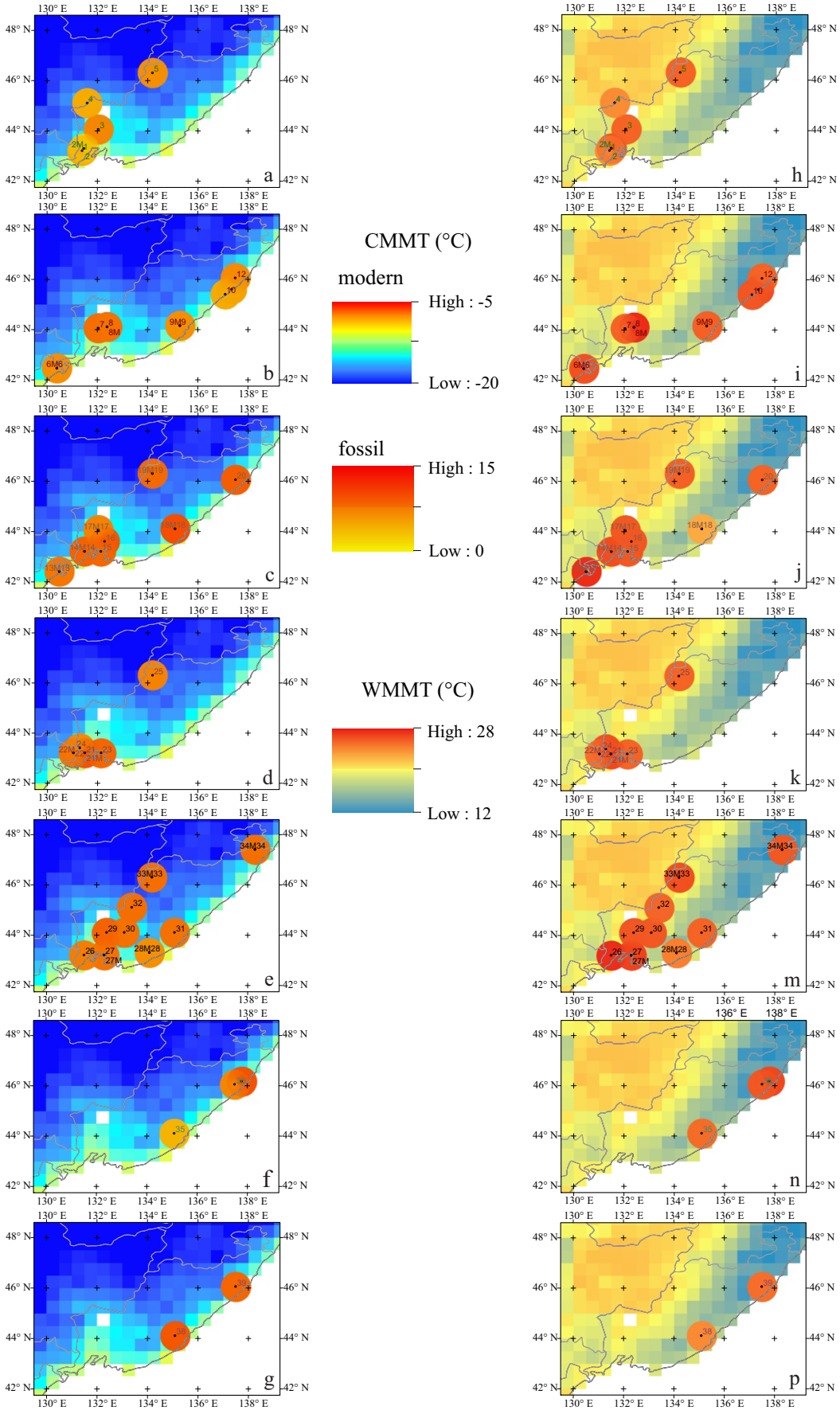

◀ **Fig. 5** CMMT (**a**–**g**) and WMMP (**h**–**p**) in the Paleogene of Primorye in comparison with modern. **a**, **h** Late Oligocene. **b**, **i** Early Oligocene. **c**, **j** Late Eocene. **d**, **k** Middle Eocene. **e**, **m** Early Eocene. **f**, **n** Late Paleocene. **g**, **p** early Paleocene. Maps are generated using ArcMAP 10.4. Modern climate data calculated from New et al. (2002). Small black discs with numbers refer to fossil sites in Table 1. Palaeoclimate data (coloured discs): interpolated means of coexistence intervals using Spatial Analyst (IDW method, power 2, and fixed search radius)

other Paleocene leaf floras indicate somewhat lower rainfall rates of the wet season (LF 38 (central part)—162 mm (88–237 mm); late Paleocene LF 35 (central part)—176 mm (116–237 mm)). Eocene MPwet attains very high values in the southeast and central part of the study area (Table 2, Fig. 6c–e); the highest value is calculated for the early Eocene PF 30 ((central part)—223 mm (205–241 mm)). In the Oligocene (Table 3, Fig. 6a, b), the highest MPwet values are indicated for the southwest of the study area (early Oligocene PF 7—236 mm (178–295 mm); late Oligocene PF 3 (southwest)—235 mm (148–322 mm)). Data obtained from for the other sites typically range from 150 to 200 mm (e.g. early Oligocene PF 6 (the southernmost flora)—151 mm (150–153 mm); late Oligocene LF 2 (southwest)—171 mm (152–191 mm)).

MPdry means in the Paleogene of Primorye were at ca. 25–35 mm in the Paleocene and Oligocene, while during the Eocene, a higher level of ca. 30–55 mm results (Table 3, Fig. 8c). The Paleocene coexistence intervals (Table 2, Fig. 6n, p) are within the range of 6–52 mm and thus at a comparatively low level. For the Eocene (Table 2, Fig. 6j, k, m), some of the floras yield higher values with MPdry > 45 mm (PF 34 (northeast)—60 mm (50–71 mm); middle Eocene PF 21 (southwest)—54 mm (45–64 mm)). At the same time, significantly lower values are reconstructed, especially for the late Eocene LF 13, located in the southwest of the study area (22 mm (7–38 mm)). In the Oligocene (Table 3, Fig. 6h, i), the highest MPdry values are indicated for sites located in the southwest (early Oligocene PF 8—54 mm (45–64 mm); late Oligocene LF 2—49 mm (43–55 mm)). However, the lowest values are reconstructed for the same region thus indicating some variability of the climate (early Oligocene PF 7 (southwest)—29 mm (18–41 mm); late Oligocene PF 3 (southwest)—27 mm (13–41 mm)).

Climate seasonality, monsoon intensity

Temperature (MART) and precipitation (MARP) seasonality parameters and the mean values of related climatic parameters for each time interval are given in Table 3 in comparison to the present-day values. The MART in the early Paleocene was 15.5 °C and gradually increased to 20.2 °C in the late Oligocene. The MARP in the early Paleocene was only 134 mm but gradually increased to 172 mm in the late Oligocene (Fig. 9a, b). The RMPwet gradually increased from 0.147 in the early Paleocene to 0.172 in the late Oligocene, while the RMPdry varied from 0.026 to 0.035 (Table 3, Fig. 9c, d).

Discussion

Differences in micro- and macro-based climate data

The integration of micro- and macrofloras in the present analysis allows for a couple of general considerations regarding resolution and quality of the obtained data thus providing clues about the integrity of the reconstruction. For the 30 microfloras, the number of taxa contributing with climate data ranged from 13 to 67 (mean 37.9, std. 12.2). The analysis of 24 macrofloras could be based on 9 to 148 (mean 42.6, std. 29.7) climate datasets of extant reference taxa. Hence, all results are considered reliable (> 10 taxa; cf. Mosbrugger and Utescher 1997), except for the early Eocene LF 33, but macrofloras better reflect past biodiversity.

Climatic requirements of 99.6% of identified NLRs of the fossil taxa in microfloras and 99.4% in macrofloras show overlapping. Generally, in 23 out of 54 cases, all NLRs can coexist, in all other cases over 96% of taxa, indicating high significance level for the results (Mosbrugger and Utescher 1997). The very high degree of overlapping in both micro- and macrofloras testifies the integrity of the NLR concepts used in each case. This is especially noteworthy when considering the fact that in a number of cases, botanical affinity was identified at a sub-generic level. Occasionally, multiple CA intervals occur at a close climatic range, possibly related to integration over differing floral horizons or caused by taphonomic effects (Utescher et al. 2014); these were combined to one single interval (cf. Online Resource 3).

As regards the MAT, the mean precision of the results, i.e. the mean width of the CA intervals for all floras amounts to 5.4 °C (std. 2.0 °C), and to 505 mm (std. 190 mm) for the MAP, respectively. When reconstructing MAT, CA intervals obtained from macrofloras are relatively narrow (mean width of CA intervals near 3.2 °C), in MAP reconstruction results are less precise (CA interval width around 415 mm at a mean). For microfloras, owing to the commonly high taxonomic level of NLR assignment resulting CA ranges are comparatively wide and provide a poorer climatic resolution. For MAT, the width of CA intervals is 6.5 °C at the mean (std. 3.1 °C). The resolution is reduced by ca. 50% when compared to the macroflora. For MAP, the width of CA intervals is also wider, 537 mm at the mean (std. 382 mm). According to Utescher et al. (2012), CA data obtained from microflora are easily capable of reflecting temporal trends due to more frequent occurrences of microfloras. However, in the majority of cases, CA data based on microfloras do not allow for quantifying minor climatic changes (Utescher et al. 2012).

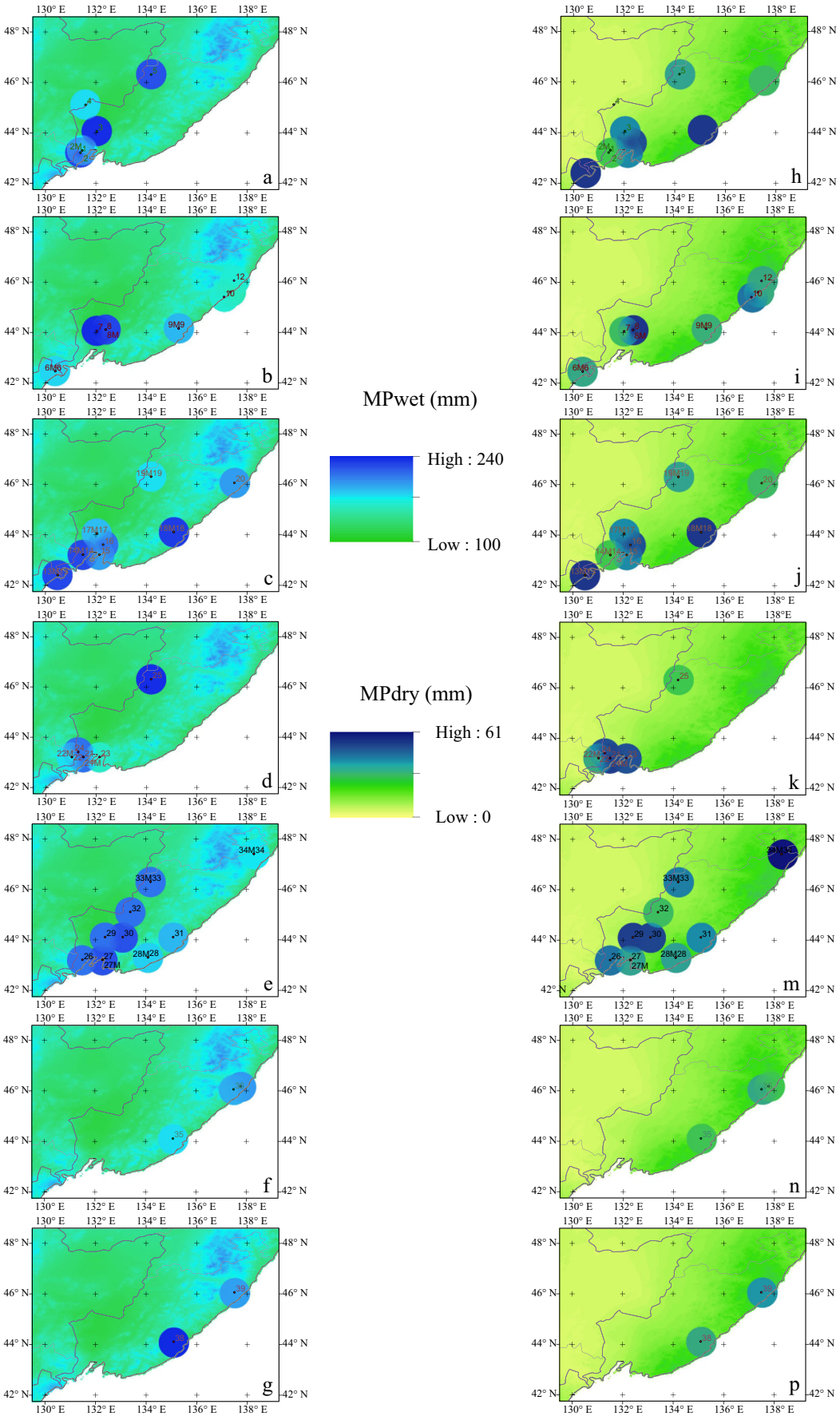

◀ **Fig. 6** MPwet (**a**–**g**) and MPdry (**h**–**p**) in the Paleogene of Primorye in comparison with modern. **a**, **h** Late Oligocene. **b**, **i** Early Oligocene. **c**, **j** Late Eocene. **d**, **k** Middle Eocene. **e**, **m** Early Eocene. **f**, **n** Late Paleocene. **g**, **p** Early Paleocene. Maps are generated using ArcMAP 10.4. Modern climate data: WorldClim–Global Climate Data (www.worldclim.org). Small black discs with numbers refer to fossil sites in Table 1. Palaeoclimate data (coloured discs): interpolated means of coexistence intervals using Spatial Analyst (IDW method, power 2, and fixed search radius)

Apart from the fact that the highest values of all climatic parameters used are related to palynofloras, no regularities in the distribution of the parameters for different organ types have been found. LF and PF from the same site and the same time interval can have different or approximately equal values for one or several climatic parameters. For example, the MAT and CMMT are higher for the PF 2 and lower for the LF 2 but WMMT is significantly higher for the LF 2 and contrary to the MAT and CMMT is lower for the PF 6 but higher for the LF 6, whereas WMMT is approximately equal (Table 2). Higher means in the microfloras can be related to the fact that identifications at genus or even species level are not possible. The larger climate ranges of genera and families, in turn, shift the CA interval means to higher values. However, all the CA intervals obtained from micro- and macrofloras overlap when the floras come from the same locality. From 54 palaeofloras studied, 15 microfloras originate from levels where macrofloras were found, and in all cases, the reconstructed climate data are largely congruent. However, the overall narrower climate ranges obtained from the mainly local macroflora tend to cover the cooler and/or drier ends of the broader ranges derived in the microflora-based reconstruction which has a lower climatic resolution and reflects regional rather than local climate. The fact that microflora-based data tend to indicate warmer conditions may be explained by a mainly northward aeolian transport of pollen grains during summer (cf. Bondarenko et al. 2013).

Spatial climatic gradients

The modern climate gradients of Primorye reflect the superimposition of the continental scale atmospheric circulation pattern such as monsoonal circulation and regional forcings. The proximity of the northern Pacific combined with the existence of a coastal mountain range with a complex relief causes a highly variable regional climate with considerable gradients, even within the same physical and geographical area. The coastal mountain range of Primorye, the Sikhote-Alin, presently attains an altitude from 500 up to 2000 m a.s.l. and plays a dual role in the distribution of both winter and summer temperatures on the northwestern and southeastern slopes (Khramtsova 1966a). It serves as a barrier preventing the free flow of cold air masses from the continent to the Sea of Japan in winter and inland transport of moist Pacific air masses thus leading to more continental, drier climate conditions in the interior and eastern part of Primorye.

When regarding the modern temperature distribution over Primorye (Figs. 4a and 5a, b), it is shown that, apart from the reflected altitudinal pattern, isotherms follow about the northeast–southwest trending Pacific coast. Lowest MATs of ca. − 1 °C are recorded in the northern part of the Sikhote-Alin Mountains while highest values of ca. 7 °C occur on the south coast. Thus, a modern MAT gradient of ca. 8 °C results for the study area extending over about 6° latitude. This gradient includes a zonal component and, more importantly, an altitudinal gradient of ca. 400–450 m (Kurentsova 1968). The modern WMMT gradient equals ca. 5 °C (ca. 17–22 °C), with the lowest values in coastal regions of the Tatar Strait in northeast of Primorye, while the highest values result for the western foothills of the Sikhote-Alin. CMMTs range from − 8 to − 14 °C along the Pacific coast, and from − 14 to − 23 °C in the inland areas. Thus, modern CMMTs display a comparatively high zonal gradient of ca. 6–9 °C and CMMT increase from coast to inland areas and the border region with China in about the same order.

The Paleogene configuration (Figs. 4a–g and 5a–p) shows significantly higher temperature levels. While WMMT was higher by ca. 5–7 °C and MAT by over 15 °C, highest anomalies with respect to present result for CMMT, attaining more than 30 °C in inland areas of Primorye. These high temperature anomalies, being most significant in the cold season, are in line with previous reconstructions of mid- to higher latitude continental temperature under the Paleogene greenhouse conditions, based on various proxies (e.g. Markwick 1994; Greenwood and Wing 1995; Utescher and Mosbrugger 2007; Greenwood et al. 2010; Utescher et al. 2011; Inglis et al. 2017). Even for the Oligocene, having a lower atmospheric CO_2, MAT anomalies in the order of 10 °C were previously reported, based on floras of the European part of the Russian Federation and Western Siberia (Popova et al. 2012) and coincide with data from marine archives (e.g. Zachos et al. 2008; Evans et al. 2018). All reconstructed temperature patterns consistently indicate that the climate was warmest throughout the Eocene and in the southeast of the study area. As regards MAT and CMMT, this feature coincides with the actual pattern. Inland sites in the 19 basins play a key role here in the comparison of past and present patterns. Unlike today, where a pointed seasonality characterises the regional climate in this area, the Paleogene climate was equable and our palaeobotany-derived CMMT and WMMT data point to a very flat gradient of a few degrees only, close to or even beyond the resolution limit of the method employed. Flat Paleogene temperature gradients at the global or continental scale have been reported earlier (e.g. Greenwood and Wing 1995). As regards the specific regional aspect, our data indicate that (1) the Sikhote-Alin Range obviously did not act as a barrier hindering the inland flow of cool air masses from the

Table 2 Mean values of climatic parameters for each palaeoflora and stratigraphic level

Stratigraphic level	Locality name	Type of flora	MAT, °C	CMMT, °C	WMMT, °C	MAP, mm	MPwet, mm	MPdry, mm	MPwarm, mm
1. Late Oligocene	1. Zanadvorovka	P	15	4.5	24	1188	225	38	148
	2. Pushkinskii9180	P	15	4.5	24	1188	225	38	148
		L	14.4	2.2	26.1	1229	171	49	126
	3. Pavlovka9035-D	P	17.1	6.6	25.6	1278	235	27	147
	4. Turii Rog8	P	15	4.5	24	1132	176	38	148
	5. Luchegorsk6212	P	16.9	6.1	25.6	1278	221	33	147
	Mean		**15.6**	**4.7**	**24.9**	**1216**	**209**	**37**	**144**
2. Early Oligocene	6. Kraskino9182/9196	P	16.9	6.1	27.4	1163	151	35	125
		L	16.3	6.1	26.2	1118	179	35	125
	7. Pavlovka9035-D	P	17.4	8.2	25.6	1278	236	29	147
	8. Rettikhovka	P	16.9	7.9	27.3	1422	226	54	148
		L	14.8	8	25.8	1329	167	32	158
	9. Voznovo9206	P	16	6.1	27.3	1323	187	33	120
		L	15.4	4.3	25.2	1134	152	35	160
	10. Tikhii Kluch	L	15.2	4.4	26	1059	160	45	130
	11. Amgu9302	L	15.4	4.8	26.3	1137	152	34	146
	12. Maksimovka	L	16.5	7.8	25.6	1126	161	34	137
	Mean		**16.1**	**6.4**	**26.3**	**1209**	**177**	**37**	**140**
3. Late Eocene	13. Gladkaya17	P	16.9	7.6	27.3	1554	226	54	147
		L	17.6	9.3	25.6	1307	212	22	154
	14. Tavrichanka9142	P	16.9	7.9	27.3	1554	226	45	147
		L	17.6	8.9	26.4	1227	225	26	147
	15. Shkotovo	P	17.6	8.5	25.9	1278	195	42	147
	16. Ivanovka610	P	18.2	9.6	26.1	1404	210	50	153
	17. Pavlovka9035-D	P	16.5	8.3	24.9	1373	187	40	160
		L	17.1	8.3	25.9	1044	186	41	108
	18. Svetlyi	P	16.3	10.2	22.9	1596	230	54	172
		L	14.8	2.2	24.6	1158	180	55	125
	19. Luchegorsk	P	16.1	6	25.5	1265	172	53	120
		L	17.2	8.3	25.7	1198	175	36	119
	20. Salibeza	L	17.5	9	25.6	1095	196	30	142
	Mean		**17**	**8**	**25.7**	**1312**	**202**	**42**	**142**
4. Middle Eocene	21. Vol'no-Nadezhdinskoe	P	16.9	7.9	27.3	1554	226	54	147
		L	17.8	9.7	26.6	1172	210	53	134
	22. Bolotnaya	P	17.4	7.8	25.2	1170	175	34	153
		L	18	9.6	26.4	1284	199	43	134
	23. Shkotovo	P	17.5	8.6	25.6	1070	156	50	129
	24. Terekhovka	P	17.3	6.5	26.2	1404	210	50	147
	25. Luchegorsk540/541	P	17.1	6.8	25.6	1278	235	27	147
	Mean		**17.4**	**8.1**	**26.1**	**1276**	**202**	**45**	**142**
5. Early Eocene	26. Tavrichanka9142	P	17.3	7.2	27.3	1554	210	45	147
	27. Smolyaninovo	P	18.2	9.6	26.2	1295	192	44	153
		L	17.5	7.9	26.8	1315	222	36	148
	28. Kluch Ugolnyi	P	18.2	8	26	1422	210	56	148
		L	17.2	6.2	24.4	1122	180	37	136
	29. Rettikhovka	P	18.2	8.9	26.1	1351	210	53	154
	30. Arsen'evka	P	18.2	8	25.9	1404	223	52	153
	31. Kluch Tuyanov	L	15.9	9	25.6	1170	187	41	160
	32. Krylovskii524	P	16.6	8.1	25.5	1278	211	29	153
	33. Luchegorsk540/541	P	16.6	8.1	26.2	1278	209	43	147
		L	15.2	5.4	24.2	1159	198	36	150
	34. Ozero Toni	P	17.4	8.2	25.9	1126	173	60	136
		L	15.1	3.9	25.9	1047	159	30	152
	Mean		**17.1**	**7.6**	**25.9**	**1271**	**199**	**43**	**149**
6. Late Paleocene	35. Ustinovka	L	16.9	3.8	25.3	1045	176	27	142
	36. Kluch Stolbikova	L	17.3	6.7	25.9	1210	190	35	145
	37. Kluch Kedrovyi	P	17.6	10	26.5	1158	197	27	127
	Mean		**17.3**	**6.8**	**25.9**	**1138**	**188**	**30**	**138**
7. Early Paleocene	38. Ustinovka	L	18.4	9.7	24.1	1045	162	34	138
	39. Sobolevka	L	14.5	8.5	25.1	1293	181	40	128
	Mean		**16.4**	**9.1**	**24.6**	**1169**	**172**	**37**	**133**

MAT, mean annual temperature; CMMT, cold month mean temperature; WMMT, warm month mean temperature; MAP, mean annual precipitation; MPwet, mean monthly precipitation of the wettest month; MPdry, mean monthly precipitation of the driest month; MPwarm, mean monthly precipitation of the warmest month

Table 3 Temperature and precipitation seasonality parameters and related values

Stratigraphic level	MATmean, °C	CMMTmean, °C	WMMTmean, °C	MART, °C	MAPmean, mm	MPwetmean, mm	MPdrymean, mm	MARP, mm	RMPwet	RMPdry
Modern	4.9	− 13.5	20.9	34.4	721	145	10	135	0.201	0.014
Late Oligocene	15.6	4.7	24.9	20.2	1216	209	37	172	0.172	0.030
Early Oligocene	16.1	6.4	26.3	19.9	1209	177	37	140	0.146	0.031
Late Eocene	17	8	25.7	17.7	1312	202	42	160	0.154	0.032
Middle Eocene	17.4	8.1	26.1	18	1276	202	45	157	0.158	0.035
Early Eocene	17.1	7.6	25.9	18.3	1271	199	43	156	0.157	0.034
Late Paleocene	17.3	6.8	25.9	19.1	1138	188	30	158	0.165	0.026
Early Paleocene	16.4	9.1	24.6	15.5	1169	172	37	135	0.147	0.032

Means by stratigraphic level (calculated using coexistence interval means)

Pacific and causing warm summers in the leeward area. Moreover, there is evidence that (2) the distribution of air pressure system during the cold season over eastern Eurasia and the related winter monsoon, today causing very low CMMTs in the inland, fundamentally differed from modern throughout the Paleogene (Takaya and Nakamura 2005; Utescher et al. 2015).

By its yearly amount of precipitation (550–920 mm), Primorye belongs to a zone with sufficient moisture and rainfall for forest vegetation. The greatest amount of precipitation, up to 800–900 mm, falls on the west coast of the Gulf of Peter the Great and in the Sikhote-Alin Mountains, on both the eastern and western slopes. In that area, MAP exceeds potential evaporation. Less humid, especially in spring and summer, are the areas of the Khanka Plain, where, with MAP at 500–600 mm, potential evaporation locally exceeds this amount. The modern MAP pattern in the study area shows a very distinct decline from coastal to inland areas (ca. 300 mm), very high MAP of > 1000 mm are confined to altitudinal areas in the northeast. Rainfall patterns of MPwet, MPwarm and MPdry have a similar structure, with MPwet ranging from ca. 50–200 mm, MPwarm from 76 to 140 mm and MPdry from almost 0–50 mm indicating seasonal drought for some inland areas (Khramtsova 1966b).

The precipitation reconstruction points to conditions considerably wetter than at present. According to our results, a distinct MAP increase in the study area occurred in the early Eocene and persists throughout the Eocene and Oligocene. High Paleogene precipitation around the globe (i.e. North and South America, Australia, Antarctica, China) is consistent with high Eocene atmospheric humidity, which would have contributed significantly to polar, and global, Eocene warming (Greenwood and Huber 2011). In the earlier Paleogene, monthly precipitation values in general are high when compared to modern conditions, broadly in accordance with the high temperatures (see above), and consistent with the general trend observed elsewhere in Eurasia from coeval records (e.g. Utescher et al. 2009; Bruch et al. 2011; Liu et al. 2011; Quan et al. 2011).

In the Paleogene of Primorye, precipitation not only was at a higher level in general compared to present-day (Figs. 4h–p and 6a–p), the pattern of regional rainfall fundamentally differed, and this holds for all studied variables: MAP, MPwet and MPdry. As far as data are available, it is shown that the inland region (Kankha Plain) and the south of Primorye were significantly more humid than today. In the early Eocene reconstruction, it is shown that inland precipitation even exceeded the values obtained from the sites presently located on the Pacific coast and therefore receiving higher rainfall. Except for the early Paleocene (MAP, MPdry) and the late Paleocene (MAP, MPwet, MPdry), there is no evidence for raised precipitation caused by an orographic gradient in the area of the

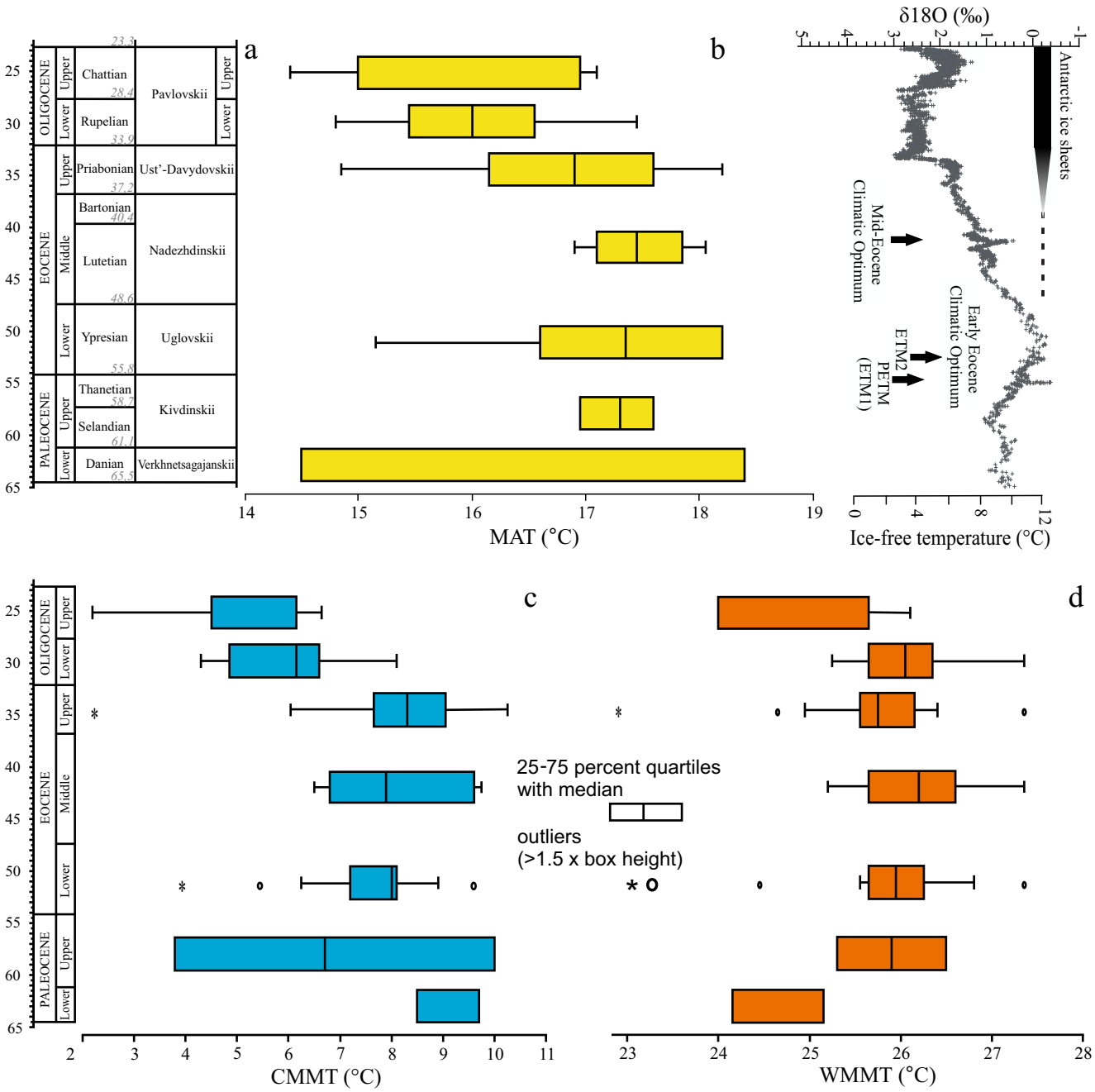

Fig. 7 MAT records (**a**) next to the composite deep-sea benthic foraminiferal oxygen isotope record after Zachos et al. (2008) (**b**), CMMT (**c**) and WMMT (**d**) records based on means of CA intervals for all palaeofloras studied. Boxplots generated using PAST 2.17

present Sikhote-Alin Range. Hence, it can be concluded that in the Paleogene, elevation of this volcanic complex was considerably lower. Also it can be inferred from the observed rainfall patterns that the main flow direction of humid air masses was from the south and southwest where the Paleogene values are among the highest (early and late Eocene, early Oligocene). This Paleogene pattern was possibly related to a monsoonal type circulation and enhanced flow of humid air masses, due to an overall flatter geomorphology of the East Asian coastal areas. A direct impact of the Pacific on coastal areas of Primorye as presently evident from the regional precipitation pattern is not visible in the Paleogene gradients. This is explained by the fact that the Paleogene coast line was located several hundred kilometres to the East (Fig. 3).

Time series

The Paleogene temperature evolution is best known from marine archives. Sea surface temperature (SST) levels in the

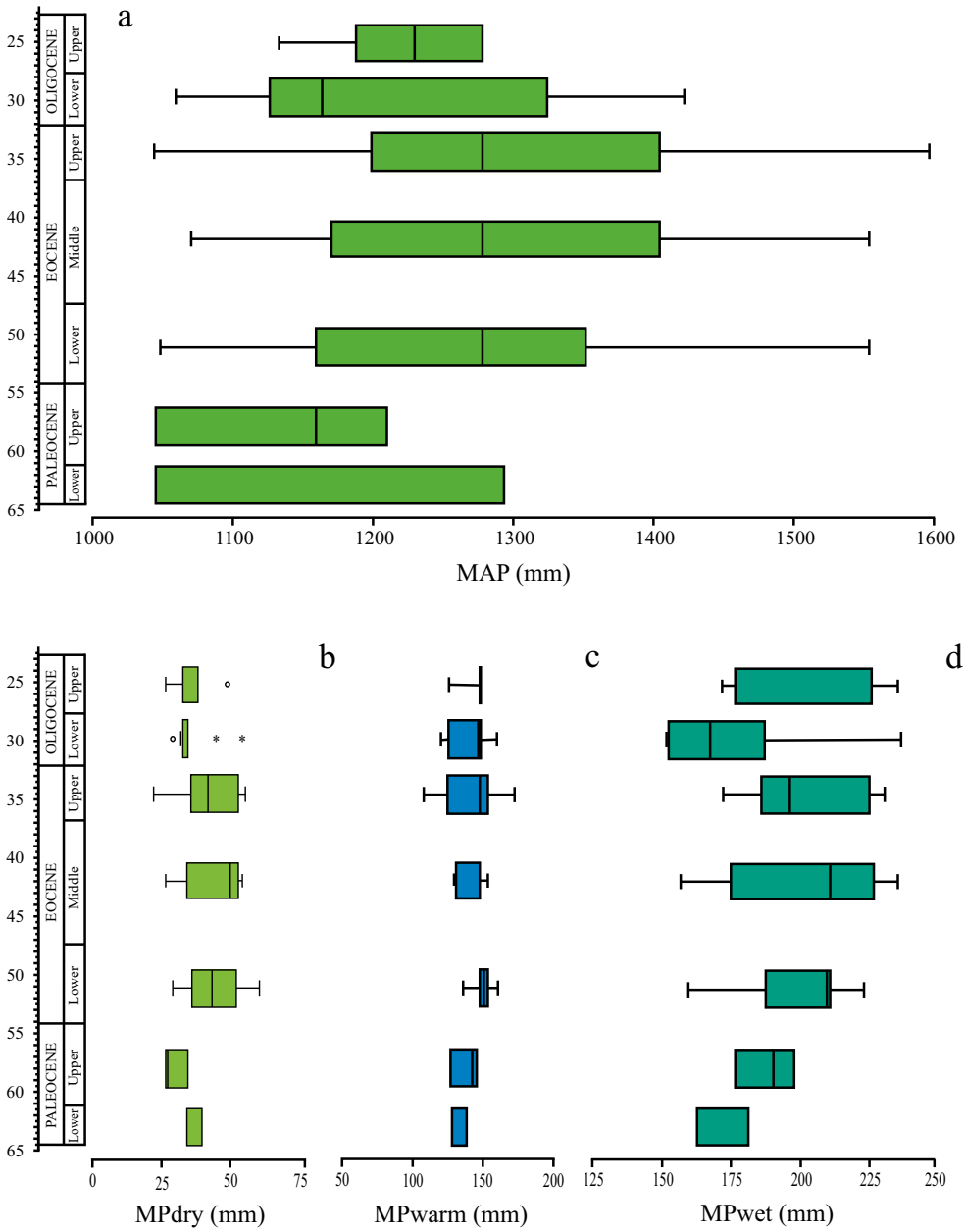

Fig. 8 MAP (**a**), MPdry (**b**), MPwet (**c**) and MPwarm (**d**) records based on means of CA intervals for all palaeofloras studied (cf. Fig. 7 for legend). Boxplots generated using PAST 2.17

Cenozoic were highest during the PETM and Eocene Thermal Maximum 2 (Wing et al. 2005; Zachos et al. 2008), and then decreased to a longer-lived climatic optimum in the middle Eocene (MECO), followed by an 'ice-house' with small ephemeral ice sheets in the early Oligocene (Zachos et al. 2008; Eldrett et al. 2009). For the continental realm, quantitative palaeoclimate reconstructions are scarce and do not cover the entire time span (Mosbrugger et al. 2005; Roth-Nebelsick et al. 2004; Quan et al. 2012; Utescher et al. 2015).

The temperature evolution over Primorye during the Paleogene in general reflects the global trend. The fossil floras studied indicate major climate change and demonstrate the general climate cooling during the Paleogene (Zachos et al. 2008). The high MAT obtained in the late Paleocene (17.3/13.1–21.4 °C) may be related to the globally high temperature level that existed at the time of the PETM while the high MAT recorded in the middle Eocene (17.4/14.7–20.2 °C) is connected to the MECO. The cooling in the late Eocene coincides with a coeval trend in the oxygen isotope record and the buildup of Antarctic ice sheets (Zachos et al. 2008). The cooling is most striking regarding the CMMT, while the same trend from the MAT record is less distinct (Fig. 7a). Thus, the present temperature reconstruction based on a total of 39

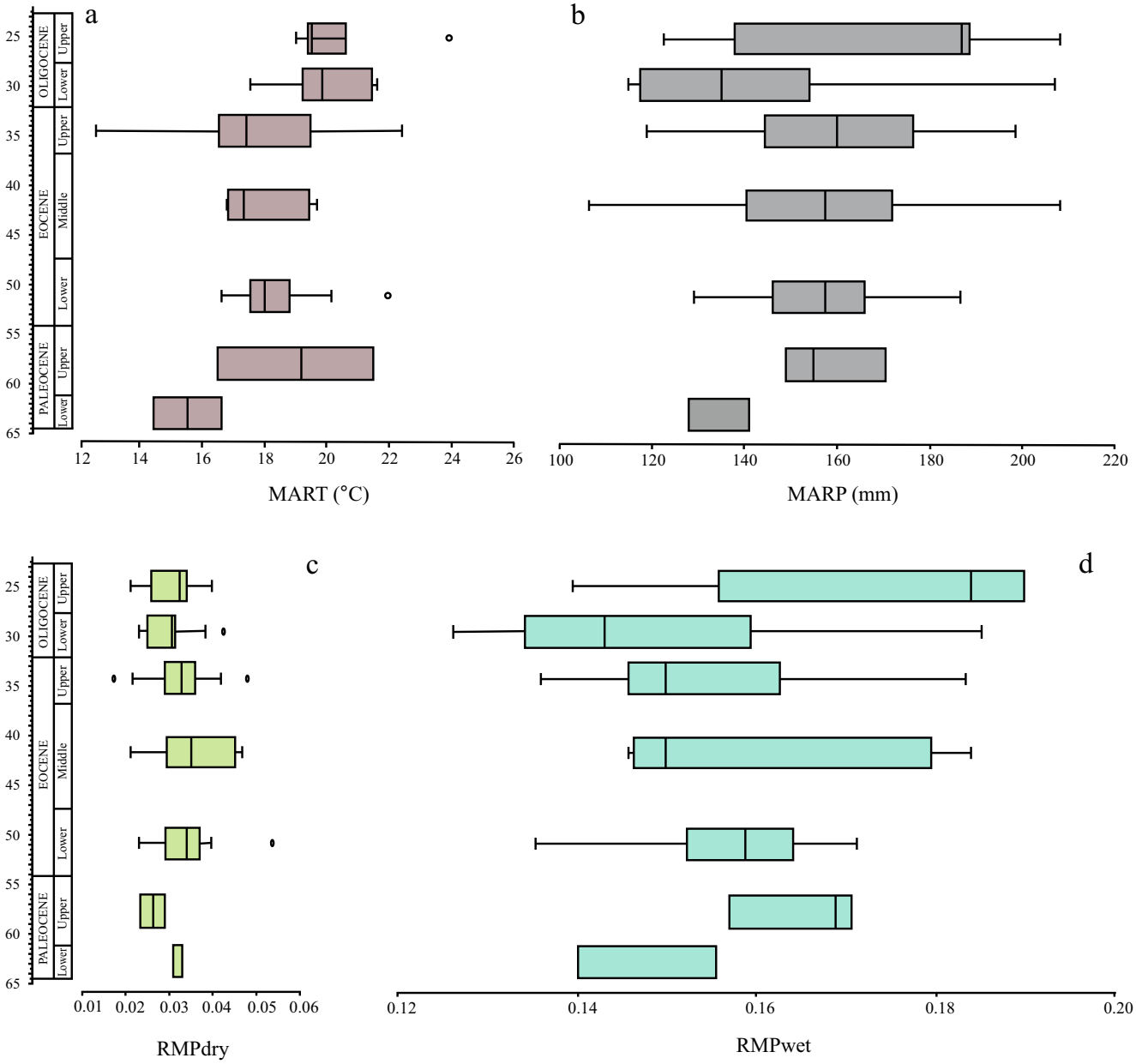

Fig. 9 MART (**a**), MARP (**b**), RMPwet (**c**) and RMPdry (**d**) records based on means of CA intervals for all palaeofloras studied (cf. Fig. 7 for legend). Boxplots generated using PAST 2.17

sites confirms the results obtained by Utescher et al. (2015) based on five floras from southern Primorye, for the time span in which both records overlap (middle Eocene to late Oligocene). Compliance of the Primorye temperature evolution since the middle Eocene and a coeval Atlantic continental record (Lusatian Basin, Lower Rhine Basin, Germany) was highlighted in Utescher et al. (2015). Another Paleogene temperature record, composed from floras recovered at Jiayin, Fushun and Shulan, is available for northeast China and thus from the closer neighbourhood of our study area (Quan et al. 2012). Features in common are the declining trend from the Paleocene to the early Eocene (CMMT), and a very warm late Eocene with subsequent distinct cooling (MAT, CMMT). The very warm late Eocene is not reflected in the global climate evolution and thus may represent a regional signal, possibly related to the initial opening of the Sea of Japan. A distinct cooling trend reported from the Fushun record (Quan et al. 2012) is not resolved in our data. According to Quan et al. (2012), among the estimated terrestrial temperature parameters, MAT slightly changed with an overall declining trend in the Eocene,

from 15.6–21.1 °C, to 17–23.9 °C, followed by 15.7–18.6 °C. However, the winter temperature dramatically decreased from 12.6–13.3 °C in the middle Eocene to 7.7–8.1 °C in the late Eocene, while the summer temperature remained almost the same with the value of 24.7–28.1 °C, 26–27.9 °C and 26.4–27.9 °C respectively in the early, middle and late Eocene. All these data are within the range of our present reconstruction or slightly higher (CMMT), respectively, which coincides with the latitude of Fushun, lower by several degrees.

Given the fact that there is a strong correlation of temperature and rainfall (cf. Spatial climatic gradients), precipitation evolution in the Paleogene of Primorye nearly follows the temperature trends, with all precipitation variables showing a pointed increasing trend from the Paleocene towards the Eocene and, thereafter, minor decline in the Oligocene. The declining trend from the Lutetian to Chattian (~ 1300 to ~ 1200 mm) was already reported in Utescher et al. (2015) based on sites of southern Primorye and can be confirmed here based on a larger set of palaeofloras, while the pointed decline of MPwet by over 50 mm in the time from the Priabonian to Chattian was apparently minor when analysing a larger plant record. Precipitation data from the adjacent continental parts in northeast China, with MAP from 735 to 1362 mm, high MPwet (means from 126 to 226 mm) and low MPdry (means from 17 to 43 mm) (Quan et al. 2012) point to a comparable evolution.

The Eocene precipitation increase in Primorye was possibly connected to the presence of first water bodies existing in the area of the later evolving Japanese back-arc basin as evidenced from the existence of late Eocene to Oligocene marine sediments along the eastern coast of the Sea of Japan (Kano et al. 2007). Another possible explanation is a link to the onset of monsoon-type circulation (see below).

Climate seasonality, monsoon intensity

Primorye presently is under the influence of the EAM (Zhang and Wang 2008). The modern regime of temperature and humidity of the territory is characterised by a pronounced seasonality. Today, MART is at the very high level of 34.4 °C, at a mean, and MARP is around 135 mm. Summer and autumn precipitation account for about 70% of the MAP, while rainfall in winter amounts to 10% only (Khramtsova 1966a, 1966b). The modern RMPwet and RMPdry, calculated based on the mean values using station data of Vladivostok (Müller and Hennings 2000; New et al. 2002), are 0.201 and 0.014, respectively (Table 3).

As mentioned above, all our climatic data suggest a strong seasonal control of the Paleogene climate of Primorye (Table 3). The higher past WMMT coupled with significantly higher CMMT indicate a lower than present seasonality of temperature during the Paleogene; however, MART gradually increased from ca 15 °C in the early Paleocene to ca. 20 °C in the late Oligocene. It should be noted that the past WMMT was only slightly higher (3.7–5.3 °C) compared to the present-day value. At the same time, the past CMMT was significantly higher compared to the present-day value: 22.6 °C higher in the early Paleocene and 18.2 °C higher in the late Oligocene.

The pronounced seasonality of precipitation (MPwet 172–209 mm; MPdry as 30–45 mm) of the Paleogene climate of Primorye gradually increased from ca. 130 mm in the early Paleocene to ca. 170 mm in the late Oligocene. Thus, the early Paleocene MARP was close to the modern but started to increase from the late Paleocene on, even attaining a higher-than-present level. However, the higher past MPwet coupled with distinctly higher MPdry indicate that, during the Paleogene, the climate of Primorye was more humid, in general.

The calculated proportions of MPwet and MPdry to yearly precipitation (MPwet: 0.147 in the early Paleocene to 0.172 in the late Oligocene; MPdry: 0.026/0.035) are almost twice as high compared to present-day (Table 3) and suggest that both, EASM and EAWM, were considerably weaker. Utescher et al. (2015) also suggest a seasonal control of precipitation in the Cenozoic climate of Primorye. According to this reconstruction, the RMPwet stayed well below the modern value until the earlier part of the late Miocene. The high RMPwet obtained by Utescher et al. (2015) for the Messinian and Piacenzian levels point to a comparatively late increasing impact of the EAM on the study area, with the Calabrian date being an outlier in this trend, indicating lower monsoon intensity at that time (Bondarenko et al. 2013).

There are vast literature resources discussing the timing of establishment of the EAM and prevalence of arid climates in the continental interior of Asia, based on various proxies that partly lead to controversial results and conclusions. For example, studies based on thick aeolian deposits in northern China (Guo et al. 2002; Qiang et al. 2011), pollen records (Sun and Wang 2005) and palaeoenvironmental patterns based on geological and geo-biological evidence (Guo et al. 2008; Wang et al. 2014b) constrained the time of the formation of the EAM to 22–25 Ma, i.e. to the Oligocene-Miocene transition. An et al. (2001) suggested that the evolution of the EAM was coupled with phased uplift of the Tibetan Plateau since the late Miocene, while others have claimed that proto-Tibetan highlands already existed throughout the Paleogene (e.g. Wang et al. 2014a; Spicer 2017), and that a monsoon-type circulation was already operational during most of the Paleogene (Huber and Goldner 2012; Hoorn et al. 2012; Quan et al. 2012, 2014; Wang et al. 2013; Licht et al. 2014; Bosboom et al. 2015). The seasonal precipitation patterns we reconstruct support the assumption of a Paleogene monsoon. The strong pulse observed in RMPwet values of our late Oligocene samples is possibly related to coeval tectonic deformation and rapid exhumation in the northwestern Tibetan Plateau and the Pamir Plateau, starting in the late Oligocene (Tada et al. 2016).

Table 4 Location of the Paleogene floras containing Larix in Primorye

Stratigraphic level	Locality name	Lon	Lat	Type of flora	References
1. Late Oligocene	Pavlovka9035-D	132.05	44.05	PF	Pavlyutkin and Petrenko 2010
2. Early Oligocene	Pavlovka9035-D	132.05	44.05	PF	Pavlyutkin and Petrenko 2010
	Rettikhovka	132.4	44.1	LF	Klimova et al. 1977
	Voznovo9206	135.3	44.15	PF, LF	Pavlyutkin et al. 2014
	Tikhii Kluch	137.1	45.4	LF	Varnavskii et al. 1988
	Maksimovka	137.5	46.05	LF	Varnavskii et al. 1988
3. Late Eocene	Luchegorsk	134.2	46.3	PF	Bolotnikova and Sedykh 1987
4. Middle Eocene	Bolotnaya	131.05	43.2	PF	Kundyshev and Petrenko 1987
5. Early Eocene	Smolyaninovo	132.3	43.2	PF	Pavlyutkin and Petrenko 2010
	Arsen'evka	133.1	44.1	PF	Bolotnikova 1988
	Luchegorsk540/541	134.2	46.3	PF	Pavlyutkin and Petrenko 2010
	Ozero Toni	138.3	47.4	LF	Varnavskii et al. 1988
6. Late Paleocene	Kluch Kedrovyi	137.78	46.17	PF	Varnavskii et al. 1988
7. Early Paleocene	–	–	–	–	–

Paleogene *Larix* record—evidence for altitudinal vegetation zones?

As mentioned above, *Larix* was excluded from climatic calculations for the Paleogene of Primorye, because it formed a cold outlier when present in the fossil record, but fossil evidence for this genus may provide valuable clues about the regional paleogene topogaphy. At present, larch grows in boreal, cold temperate regions of the Northern Hemisphere, including Europe, Asia and North America (Kharkevich 1989; FNA Editorial Committee 1993; Wu and Raven 1999) and thus, its presence in the warm temperate phytocoenoses existing in the Paleogene of Primorye is in need of further considerations. At present, larch occurs from the Pacific coast of Primorye to the tree line at higher altitudes; however, in the southwest of the study area, the genus is less common, whereas in the northeast, it is one of the major forest-forming trees (Kharkevich 1989). Larch grows at the (0)300–4300(4600) m a.s.l., mainly in mountains, hills, slopes, rare in swamps, valleys and lowland subarctic plains (Kharkevich 1989; FNA Editorial Committee 1993; Wu and Raven 1999).

Paleogene floras of Primorye containing larch remains are listed in Table 4. While *Larix* was absent from the early Paleocene floras, the earliest records of *Larix* pollen are known from the late Paleocene floras in the northeast of the territory. In the Eocene, *Larix* pollen and even macro-remains are reported from various sites located in the north and northeast of the study area while for the middle Eocene, *Larix* pollen are also described from several localities of the southwest.

The concentration of *Larix* records in the northeast of the study area was probably related to uplift processes in the area of the present-day Sikhote-Alin Range (Fig. 3) that were connected with coeval volcanic activities. The elevation may have exceeded 500 m a.s.l. (Akhmetiev et al. 2009), and it is assumed that this was already sufficient for the manifestation of altitudinal vegetation zones (Blokhina 1987). Thus, it may be assumed, that in the Paleogene, the larch was, most likely, an element of extrazonal altitudinal vegetation. Since the early Oligocene and in the Neogene (cf. Bobrov 1972; Blokhina 1999, 2012), *Larix* became more abundant and widespread in the pollen record of Primorye, probably linked to the observed general cooling trend and/or uplift processes.

Conclusions

The exceptionally rich palaeobotanical record of Primorye holds the key for reconstructing the detailed Paleogene regional climate evolution in space and time, and to trace potentially monsoon-induced patterns. The high diversity of the palaeofloras and up-to-date taxonomy result in useful climatic interpretations. Our climate maps for the first time allow quantifying climate change in space and time on the Pacific side of Eurasia over the Paleogene. The climate curves of Primorye are consistent with major global trends, indicate major climate changes and demonstrate the general climate cooling during the Paleogene. The cooling is most striking regarding the CMMT, the same trend from the MAT record is less distinct. Our temperature reconstruction for the Paleogene of Primorye points to significantly warmer conditions than at present. All inferred temperature patterns consistently indicate that the climate was warmest throughout the Eocene and in the southeast of the study area. The high temperature anomalies, being most distinct as regards the cold season, are in line with previous reconstructions of mid- to higher latitude continental temperature under

the Paleogene greenhouse conditions based on various proxies. At the same time, flat Paleogene temperature gradients of Primorye have been related to the specific regional aspects (1) the Sikhote-Alin Range obviously did not act as a barrier hindering the landward flow of cool air masses from the Pacific and causing warm summers in the leeward area and (2) the distribution of air pressure system during the cold season over eastern Eurasia and the related winter monsoon fundamentally differed from modern throughout the Paleogene. The precipitation reconstruction points to conditions considerably wetter than at present. According to our results, a distinct increase in MAP is observed in the early Eocene and persists throughout the Eocene and Oligocene. Moreover, in the Paleogene of Primorye, precipitation not only was at a higher level in general compared to present-day, the pattern of regional rainfall fundamentally differed, and this holds for all studied variable and shows that the inland region (Khanka Plain) and the south of Primorye were significantly more humid than today. There is no evidence for raised precipitation caused by the modern orographic gradient of the Sikhote-Alin Range. It can be concluded that in the Paleogene, elevation of this volcanic complex was considerably lower and be inferred from the observed rainfall patterns that the main flow direction of humid air masses was from the south and southwest where the Paleogene values are among the highest. This Paleogene pattern was possibly related to a monsoon-type circulation and enhanced flow of humid air masses, due to an overall flatter geomorphology of the East Asian coastal areas.

Acknowledgements The authors are thankful to an anonymous reviewer and Prof. Christopher Yusheng Liu for carefully revising the manuscript and for their valuable suggestions.

The study was supported by the Russian Foundation for Basic Research (project no. 16-04-01241) to Nadezhda I. Blokhina. This work is a contribution to NECLIME (Neogene Climate Evolution in Eurasia).

Compliance with ethical standards

Conflict of interest The authors declare that they have no conflict of interest.

References

Abels, H. A., Dupont-Nivet, G., Xiao, G., Bosboom, R., & Krijgsman, W. (2011). Step-wise change of Asian interior climate preceding the Eocene–Oligocene Transition (EOT). *Paleogeography, Paleoclimatology, Paleoecology, 299*, 399–412.

Ablaev, A. G. (1977). Flora uglenosnykh neogenovykh otlozhenii Primor'ya. In V. G. Varnavskii (Ed.), *Stratigrafiya kainozoiskikh otlozhenii Dal'nego Vostoka* (pp. 54–58). Vladivostok: Izdatel'stvo DVNTs AN SSSR [in Russian].

Ablaev, A. G. (2000). *Paleogene biostratigraphy of the coastal region in south Primor'e*. Vladivostok: Dal'nauka [in Russian].

Ablaev, A. G., & Akhmetiev, M. A. (1977). Bolotninskaya miotsenovaya flora Yuzhnogo Primor'ya i rol' v ee sostave teplolyubivykh elementov. *Paleontologicheskii Zhurnal, 1*, 134–141 [in Russian].

Ablaev, A. G., Li, C. S., Vassiliev, I. V., & Wang, Y. F. (2005). *Paleogene of the eastern Sikhote-Alin*. Vladivostok: Dal'nauka [in Russian].

Ablaev, A. G., Li, C. S., & Wang, Y. F. (2006). *Paleogene of the Bikin-Ussuri Basin sedimentation (Lower-Bikin depression)*. Vladivostok: Dal'nauka [in Russian].

Akhmetiev, M.A. (1973). Miotsenovaya flora Sikhote-Alinya (Trudy GIN AN SSSR, Vol. 247). Moscow: GIN AN SSSR. [in Russian].

Akhmetiev, M. A. (1988). *Kainozoiskie flory vostochnogo Sikhote-Alinya*. Moscow: GIN AN SSSR [in Russian].

Akhmetiev, M.A. (2004). The Paleocene and Eocene global climate. Paleobotanical evidences. In M.A. Semikhatov & N.M. Chumakov (Eds.), Climate in the epoches of major biospheric transformations (Trudy GIN AN SSSR, Vol. 550) (pp. 10–43). Moscow: GIN AN SSSR. [in Russian].

Akhmetiev, M. A. (2015). High-latitude regions of Siberia and northeast Russia in the Paleogene: Stratigraphy, flora, climate, coal accumulation. *Stratigraphy and Geological Correlation, 23*(4), 421–435.

Akhmetiev, M. A., Bolotnikova, M. D., Bratseva, G. M., & Krassilov, V. A. (1978). Stratigrafiya i paleofloristika opornogo razreza kainozoya Yuzhnogo Primor'ya. *Izvestiya AN SSSR. Ser. Geol, 4*, 61–75 [in Russian].

Akhmetiev, M. A., Bratseva, G. M., & Klimova, R. S. (1973). O vozrastnykh analogakh engelgardievykh sloev Korei v Primor'e. *Doklady AN SSSR, 209*(1), 167–170 [in Russian].

Akhmetiev, M. A., & Shyvareva, N. A. (1989). Iskopaemye golosemennye Amgu (Vostochnyi Sikhote-Alin'). In M. A. Akhmetiev (Ed.), *Paleofloristika i stratigrafiya fanerozoya* (pp. 104–117). Moscow: GIN AN SSSR [in Russian].

Akhmetiev, M. A., & Zaporozhets, N. I. (2017). The climate-forming role of Early Paleogene marine currents in high latitudes of Eurasia. *Stratigraphy and Geological Correlation, 25*(2), 229–240.

Akhmetiev, M., Walther, H., & Kvacek, Z. (2009). Mid-latitude Palaeogene floras of Eurasia bound to volcanic settings and palaeoclimatic events—experience obtained from the Far East of Russia (Sikhote-Alin') and Central Europe (Bohemian Massif). *Acta Musei Nationalis Pragae, Series B - Historia Naturalis, 65*, 61–129.

An, Z. S., Kutzbach, J. E., Prell, W. L., & Porter, S. C. (2001). Evolution of Asian monsoons and phases uplift of the Himalayan Tibetan Plateau since Late Miocene times. *Nature, 411*, 62–66.

Baskakova, L. A., & Gromova, N. S. (1979). Biostratigraficheskoe raschlenenie uglovskogo gorizonta po palinologicheskim dannym. In B. V. Poyarkov (Ed.), *Paleontologia i stratigrafiya Dal'nego Vostoka* (pp. 109–114). Vladivostok: Izdatel'stvo DVNTs AN SSSR [in Russian].

Baskakova, L. A., & Gromova, N. S. (1982). Fitostratigraficheskoe raschlenenie paleogenovykh otlozhenii Yugo-Zapadnogo Primor'ya. *Sovetskaya Geologia, 11*, 68–78 [in Russian].

Baskakova, L. A., & Gromova, N. S. (1984). Stratigrafiya Smolyaninovskogo ugol'nogo razreza v Yuzhnom Primor'e. In A. G. Ablaev (Ed.), *Materialy po stratigrafii i paleogeografii Vostochnoi Azii* (pp. 59–69). Vladivostok: Izdatel'stvo DVNTs AN SSSR [in Russian].

Baskakova, L. A., & Lepekhina, V. G. (1990). Novye dannye po fitostratigrafii paleogena Zerkal'nenskoi vpadiny. In A. G. Ablaev (Ed.), *Novye dannye po stratigrafii Dal'nego Vostoka i Tikhogo okeana* (pp. 52–60). Vladivostok: Izdatel'stvo DVO RAN [in Russian].

Bijl, P. K., Schouten, S., Sluijs, A., Reichart, G.-J., Zachos, J. C., & Brinkhuis, H. (2009). Early Palaeogene temperature evolution of the southwest Pacific Ocean. *Nature, 461*, 776–779.

Blokhina, N. I. (1987). An attempt of reconstruction of relief and plant communities of the past using xylotomic data. *Botanicheskii Zhurnal, 72*(2), 197–201 [in Russian].

Blokhina, N.I. (1999). Fossil larches of the Sikhote-Alin. In Yu.I. Man'ko (Ed.), Forest and forest formation process in the Far East: Proceedings of International Conference, devoted to the 90-th anniversary of B.P. Kolesnikov (pp. 170–171). Vladivostok: IBSS DVO RAN. [in Russian].

Blokhina, N.I. (2012). The origin and possible ways of distribution of the Far Eastern larches by palaeobotanical data. In M.A. Akhmetiev et al. (Eds.), Biogeography: Methodology, regional and historical aspects: Proceedings of the conference dedicated to the 80-th anniversary of V.N. Tikhomirov (1932–1997) (pp. 41–44). Moskow: KMK Scientific Press. [in Russian].

Bobrov, E. G. (1972). Istoriya i sistematika listvennits. *Komarovskie chteniya, 25*, 1–96 [in Russian].

Bolotnikova, M. D., & Sedykh, A. K. (1987). Novye dannye po stratigrafii uglenosnykh otlozhenii Nizhnebikinskoi vpadiny. In V. A. Markevich (Ed.), *Palinologiya Vostoka SSSR* (pp. 41–52). Vladivostok: Izdatel'stvo DVNTs AN SSSR [in Russian].

Bolotnikova, T. N. (1988). Palinologicheskaya kharakteristika i vozrast uglenosnykh otlozhenii Chernyshevskogo burougol'nogo mestorozhdenia (Yuzhnoe Primor'e). *Tikhookeanskaya geologia, 4*, 101–105 [in Russian].

Bolotnikova, T. N. (1993). Palinologicheskaya kharakteristika uglenosnykh otlozhenii Vostochnogo uchastka Pavlovskogo mestorozhdenia. *Tikhookeanskaya geologia, 6*, 102–110 [in Russian].

Bolotnikova, T. N. (1994). Palinostratigrafiya kainozoiskikh otlozhenii Pavlovskogo burougol'nogo mestorozhdenia. *Tikhookeanskaya geologia, 1*, 71–81 [in Russian].

Bondarenko, O. V., Blokhina, N. I., & Utescher, T. (2013). Quantification of Calabrian climate in southern Primory'e, Far East of Russia—an integrative case study using multiple proxies. *Palaeogeography, Palaeoclimatology, Palaeoecology, 386*, 445–458.

Borsuk, M. O. (1952). *Iskopaemaya flora verkhnemelovykh otlozhenii Primor'ya*. Moskva: Gosgeoltekhizdat [in Russian].

Bosboom, R., Mandic, O., Dupont-Nivet, G., Proust, J.N., Ormukov, C., & Aminov, J. (2015). Late Eocene palaeogeography of the proto-Paratethys Sea in Central Asia (NW China, southern Kyrgyzstan and SW Tajikistan). In M.F. Brunet, T. McCann & E.R. Sobel (Eds.), *Geological Evolution of Central Asian Basins and the Western Tien Shan Range* (Special Publications, 427 pp.). London: Geological Society.

Bruch, A. A., Utescher, T., & Mosbrugger, V. (2011). Precipitation patterns in the Miocene of Central Europe and the development of continentality. *Palaeogeography, Palaeoclimatology, Palaeoecology, 304*, 202–211.

Budantsev, L.Yu. (1997). *Pozdneeotsenovaya flora Zapadnoi Kamchatki* (Trudy BIN RAN, 19). Sankt-Peterburg: Izdatel'stvo "Petro-RIF". [in Russian].

Budantsev, L. Y. (1999). The reconstruction of the Cenozoic climates in eastern-north Asia based on palaeobotanical data. *Botanicheskii Zhurnal, 84*(10), 36–45 [in Russian].

Chashchin, A. A., Popov, V. K., Nechaev, V. P., Chekryzhov, I., Yu, Nechaeva, M. G., & Blokhin, M. G. (2013). Geokhimicheskie osobennosti eotsenovogo vulkanizma riftogennykh vpadin Yugo-Zapadnogo Primor'ya. In S. V. Rasskazov et al. (Eds.), *Kontinental'nyi riftogenez, soputstvuyutshie protsessy* (pp. 164–168). Irkutsk: Institute of the Earth's Crust SO RAN and Irkutsk State University [in Russian].

Chekryzhov, I. Y., Popov, V. K., Panichev, A. M., Seredin, V. V., & Smirnova, E. V. (2010). Novye dannye po stratigrafii, vulkanizmu i tseolitovoi mineralizatsii kainozoiskoi vanchinskoi vpadiny, Primorskii krai. *Tikhookeanskaya geologia, 29*(4), 45–63 [in Russian].

Cohen, K. M., Finney, S. M., Gibbard, P. L., & Fan, J. X. (2013). The ICS international chronostratigraphic chart. *Episodes, 36*, 199–204.

Denisov, E. P. (1965). *Noveishaya tektonica i pozdnekainozoiskii vulkanizm Yuzhnogo Primor'ya*. Vladivostok: Dal'nevostochnoe knizhnoe Izdatel'stvo [in Russian].

Dupont-Nivet, G., Krijgsman, W., Langereis, C., Abels, H. A., Dai, S., & Fang, X. (2007). Tibetan plateau aridification linked to global cooling at the Eocene–Oligocene transition. *Nature, 445*, 635–638.

Eldrett, J. S., Greenwood, D. R., Harding, I. C., & Huber, M. (2009). Increased seasonality through the Eocene to Oligocene transition in northern high latitudes. *Nature, 459*, 969–973.

Evans, D., Sagoo, N., Renema, W., Cotton, L. J., Müller, W., Todd, J. A., Saraswati, P. K., Stassen, P., Ziegler, M., Pearson, P. N., Valdes, P. J., & Affek, H. P. (2018). Eocene greenhouse climate revealed by coupled clumped isotope-Mg/Ca thermometry. *Proceedings of the National Academy of Sciences, 115*(6), 1174–1179.

Fang, J., Wang, Z., & Tang, Z. (2009). Atlas of woody plants in China. Vol. 1 and Index. Beijing: Higher Education Press.

Fang, J., Wang, Z., & Tang, Z. (2011). Atlas of woody plants in China. Vol. 2 and Index. Beijing: Higher Education Press.

Flerov, K. K., Belyaeva, E. I., Yanovskaya, N. M., Gureev, A. A., Novodvorskaya, I. M., Kornilova, V. S., Shevyreva, N. S., Kurochkin, E. N., Zherikhin, V. V., Chkhikvadze, V. M., Martinson, G. G., Tolstikova, N. V., Chepalyga, A. L., & Fotjanova, L. I. (1974). *Zoogeography of Palaeogena Asia (Trudy PIN AN SSSR, 146)*. Moskow: Nauka [in Russian].

FNA Editorial Committee (Eds.) (1993). *Flora of North America North of Mexico*. vol. 2 (Pteridophytes and Gymnosperms). New York and Oxford: Oxford University Press.

Gallagher, S.J., Wallace, M.W., Li, C.L., Kinna, B., Bye, J.T., Akimoto, A., & Torii, M. (2009). Neogene history of the West Pacific Warm Pool, Kuroshio and Leeuwin currents. *Paleoceanography* 24, doi: https://doi.org/10.1029/2008PA001660.

Gerasimov, I. P. (Ed.). (1969). *Prirodnye usloviya i estestvennye resursy SSSR. Uzhnaya chast' Dal'nego Vostoka*. Moskva: Nauka [in Russian].

Golozubov, V. V. (2006). *Tectonics of the jurassic and lower cretaceous complexes of the north-western framing of the Pacific Ocean*. Vladivostok: Dal'nauka [in Russian].

Greenwood, D. R., & Wing, S. L. (1995). Eocene continental climates and latitudinal temperature gradients. *Geology, 23*, 1044–1048.

Greenwood, D. R., Basinger, J. F., & Smith, R. Y. (2010). How wet was the Arctic Eocene rain forest? Estimates of precipitation from Paleogene Arctic macrofloras. *Geology, 38*, 15–18.

Greenwood, D.R., & Huber, M. (2011). Eocene precipitation: A global monsoon? *American Geophysical Union, Fall Meeting 2011*, abstract id. T22C-07.

Gromova, N.S. (1980). Palinokompleks nazimovskoi svity Yuzhnogo Primor'ya. Paleomikrofitologicheskie issledovaniya dlya tselei stratigrafii. *Trudy VSEGEI*. Nov. ser. 305, 80–83. [in Russian].

Guo, Z. T., Ruddiman, W. F., Hao, Q. Z., Wu, H. B., Qiao, Y. S., Zhu, R. X., Peng, S. Z., Wei, J. J., Yuan, B. Y., & Liu, T. S. (2002). Onset of Asian desertification by 22 Myr ago inferred from loess deposits in China. *Nature, 416*, 159–163.

Guo, Z. T., Sun, B., Zhang, Z. S., Peng, S. Z., Xiao, G. Q., Ge, J. Y., Hao, Q. Z., Qiao, Y. S., Liang, M. Y., Liu, J. F., Yin, Q. Z., & Wei, J. J. (2008). A major reorganization of Asian climate by the early Miocene. *Climate of the Past, 4*, 153–174.

Hao, H., Ferguson, D. K., Feng, G. P., Ablaev, A., Wang, Y. F., & Li, C. S. (2010). Early Paleocene vegetation and climate in Jiayin, NE China. *Climatic Change, 99*, 547–566.

He, C. X., & Tao, J. R. (1997). A study on the Eocene flora in Yilan County, Heilongjiang. *Acta Phytotaxonomica Sinica, 35*, 249–256.

Hirooka, K. (1990). Paleomagnetic studies of Pre-Cretaceous rocks in Japan. *Publ. of IGSP Project, 224*, 401–406.

Hoorn, C., Straathof, J., Abels, H. A., Hu, Y. D., Utescher, T., & Dupont-Nivet, G. (2012). A late Eocene palynological record of climate change and Tibetan Plateau uplift (Xining Basin, China). *Palaeogeography, Palaeoclimatology, Palaeoecology, 344–345*, 16–38.

Huber, M., & Goldner, A. (2012). Eocene monsoons. *Journal of Asian Earth Sciences, 44*, 3–23.

Inglis, G. N., Collinson, M. E., Riegel, W., Wilde, V., Farnsworth, A., Lunt, D. J., Valdes, P., Robson, B. E., Scott, A. C., Lenz, O. K., Naafs, B. D. A., & Pancost, R. D. (2017). Mid-latitude continental temperatures through the early Eocene in western Europe. *Earth and Planetary Science Letters, 460*, 86–96.

Jacques, F. M. B., Gou, S. X., Su, T., Xing, Y. W., Huang, Y. J., Li, Y. S., Ferguson, D. K., & Zhou, Z. (2011). Quantitative reconstruction of the Late Miocene monsoon climates of southwest China: A case study of the Lincang flora from Yunnan Province. *Palaeogeography, Palaeoclimatology, Palaeoecology, 304*, 318–327.

Jolley, D. W., & Widdowson, M. (2005). Did Paleogene North Atlantic rift-related eruptions drive early Eocene climate cooling? *Lithos, 79*, 355–366.

Kano, K., Uto, K., & Oguchi, T. (2007). Stratigraphic review of Eocene to Oligocene successions along the eastern Japan Sea: Implication for early opening of the Japan Sea. *Journal of Asian Earth Sciences, 30*(1), 20–32.

Kawai, N., Kume, S., & Ito, H. (1962). Study on the magnetisation of the Japanese rocks. *Journal of Geomagnetism and Geoelectricity, 13*, 150–203.

Kharkevich, S.S. (Ed.) (1989). *Sosudistye rasteniya sovetskogo Dal'nego Vostoka*. Tom 4, Leningrad: Nauka. [in Russian].

Khramtsova, V.K. (Ed.) (1966a). *Spravochnik po klimatu SSSR*. vyp. 26, Primorskii krai. Chast' 2. Temperatura vozdukha i pochvy. Leningrad: Gidrometeoizdat. [in Russian].

Khramtsova, V.K. (Ed.) (1966b). *Spravochnik po klimatu SSSR*. vyp. 26, Primorskii krai. Chast' 4. Vlazhnost' i osadki. Leningrad: Gidrometeoizdat. [in Russian].

Khudyakov, G. I., Denisov, E. P., Korotkii, A. M., Kulakov, A. P., Nikonova, R. I., & Chernobrovkina, E. I. (1972). *Yug Dal'nego Vostoka. Istoriya razvitiya rel'efa Sibiri i Dal'nego Vostoka*. Moskow: Nauka [in Russian].

Klimova, R. S. (1981). Novyi vid Acer iz miotsena Severo-Vostochnogo Primor'ya. *Paleontologicheskii Zhurnal, 1*, 134–138 [in Russian].

Klimova, R. S. (1988). Nekotorye predstaviteli teplolyubivykh rastenii iz miotsena Primorskogo kraya. *Paleontologicheskii Zhurnal, 1*, 92–99 [in Russian].

Klimova, R.S., Kramchanin, A.F., & Demidova, T.I. (1977). Novye dannye po stratigrafii Rettikhovskogo uglenosnogo razreza. In V.G. Varnavskii (Ed.), Stratigrafiya kainozoiskikh otlozhenii Dal'nego Vostoka (pp. 66–75). Vladivostok: Izdatel'stvo DVNTs AN SSSR. [in Russian].

Klimova, R. S., & Tsar'ko, E. I. (1989). O nakhodke paleogenovykh rastenii i diatomei v salibezskoi toltshee basseina reki Svetlovodnaya (Severo-Vostochnoe Primor'e). In V. A. Krassilov & R. S. Klimova (Eds.), *Kainozoi Dal'nego Vostoka* (pp. 57–63). Vladivostok: Izdatel'stvo DVO AN SSSR [in Russian].

Kolesov, E. V. (2003). Paleotektonicheskaya evolutsiya Severo-Vostochnogo regiona Rossii po paleomagnitnym dannym. In S. G. Byalobzheskii et al. (Eds.), *Materialy vserossiiskogo sovetshaniya* "*Geodinamika, magmatizm i mineralogeniya kontinental'nykh okrain Severnoi Patsifiki*" (pp. 101–102). Magadan: Izdatel'stvo SVKNII [in Russian].

Koshman, M. M. (1964). Retichnaya flora Bikinskogo burougol'nogo mestorozhdenia. *Botanicheskii Zhurnal, 49*(2), 265–271 [in Russian].

Krassilov, V. A. (1989). Smena flory na granites mela i paleogena v Kavalerovskom raione, Primor'e. In V. A. Krassilov & R. S. Klimova (Eds.), *Kainozoi Dal'nego Vostoka* (pp. 34–37). Vladivostok: Izdatel'stvo DVO AN SSSR [in Russian].

Kropotkin, P. N., & Shakhvarstova, K. A. (1965). *Geologicheskoe stroenie tikhookeanskogo podvizhnogo poyasa*. Moskow: Nauka [in Russian].

Kundyshev, A. S., & Petrenko, T. I. (1987). O vozraste bolotninskoi iskopaemoi flory Yuzhnogo Primor'ya. In V. A. Markevich (Ed.), *Palinologia vostoka SSSR* (pp. 53–59). Vladivostok: Izdatel'stvo DVNTs AN SSSR [in Russian].

Kundyshev, A. S., & Verkhovskaya, N. B. (1989). O vozraste uglenosnykh otlozhenii Nizhnebikinskoi vpadiny. In V. A. Krassilov & R. S. Klimova (Eds.), *Kainozoi Dal'nego Vostoka* (pp. 121–127). Vladivostok: Izdatel'stvo DVO AN SSSR [in Russian].

Kurentsova, G. E. (1968). *Rastitel'nost' Primorskogo kraya*. Vladivostok: Dal'nevostochnoe knizhnoe izdatel'stvo [in Russian].

Lebedeva, N. A. (1957). Geomorfologia, neogen-chetvertichnye otlozheniya i neotektonika zapadnoi chaste Yuzhnogo Primor'ya (Prikhankaiskii raion). In Editorial Committee (Ed.), *Trudy Komissii po izucheniyu chetvertichnogo perioda AN SSSR* (Vol. 13, pp. 221–227). Moskow: Izdatel'stvo AN SSSR [in Russian].

Lee, G., Besse, J., Courilott, V., & Montigny, R. (1987). Eastern Asia in Cretaceous: New paleomagnetic data from South Korea and a new look at Cninese and Japanese data. *Journal Geophysical Research, 92*, 3580–3596.

Licht, A., Van Cappelle, M., Abels, H. A., Ladant, J. B., Trabucho-Alexandre, J., France-Lanord, C., Donnalieu, Y., Vandenberghe, J., Rigaudier, T., Lécuyer, C., Terry, D., Jr., Adriaens, R., Boura, A., Guo, Z., Soe, A. N., Quade, J., Dupont-Nivet, G., & Jaeger, J. J. (2014). Asian monsoons in a late Eocene greenhouse world. *Nature, 513*, 501–506.

Liu, X. D., & Yin, Z. Y. (2002). Sensitivity of East Asian monsoon climate to the uplift of the Tibetan Plateau. *Palaeogeography, Palaeoclimatology, Palaeoecology, 183*, 223–245.

Liu, J., Wang, B., Wang, H., Kuang, X., & Ti, R. (2011). Forced response of the East Asian summer rainfall over the past millennium: Results from a coupled model simulation. *Climate Dynamics, 36*, 323–336.

Liu, X., Guo, Q., Guo, Z., Yin, Z. Y., Dong, B., & Smith, R. (2015). Where were the monsoon regions and arid zones in Asia prior to the Tibetan Plateau uplift? *National Science Review, 2*(4), 403–416.

Markwick, P. J. (1994). "Equability", continentality and Tertiary "climate": The crocodilian perspective. *Geology, 22*, 613–616.

Maruyama, S., Isozaki, Y., Kimura, G., & Terabayashi, M. (1997). Paleogeographic maps of the Japanese Islands: Plate tectonic synthesis from 750 Ma to the present. *The Island Arc, 6*, 121–142.

Matthiessen, J., Knies, J., Vogt, C., & Stein, R. (2009). Pliocene palaeoceanography of the Arctic Ocean and subarctic seas. *Philosophical Transactions of the Royal Society of London. Series A, 367*, 21–48.

Mikhailov, V. A., Feoktistov, Y. M., & Klimova, R. S. (1989). Novye dannye po fitostratigrafii kainozoya vostochnoi chaste Zerkal'nenskoi depressii. In V. A. Krassilov & R. S. Klimova (Eds.), *Kainozoi Dal'nego Vostoka* (pp. 38–49). Vladivostok: Izdatel'stvo DVO AN SSSR [in Russian].

Mosbrugger, V., & Utescher, T. (1997). The coexistence approach—A method for quantitative reconstructions of Tertiary terrestrial palaeoclimate data using plant fossils. *Paleogeography, Palaeoclimatology, Palaeoecology, 134*, 61–86.

Mosbrugger, V., Utescher, T., & Dilcher, D. (2005). Cenozoic continental climatic evolution of Central Europe. *Proceedings of the National Academy of Sciences, 102*(42), 14964–14969.

Müller, M. J., & Hennings, D. (2000). *The global climate data atlas on CD Rom*. Flensburg: University Flensburg, Institute für Geografie.

New, M., Lister, D., Hulme, M., & Makin, I. (2002). A high-resolution data set of surface climate over global land areas. *Climate Research, 21*, 1–25.

Oleinikov, A. V., & Klimova, R. S. (1977). Novye dannye po stratigrafii neogenovykh vulkanogennykh otlozhenii basseina reki Samarga. In V. G. Varnavskii (Ed.), *Stratigrafiya kainozoiskikh otlozhenii Dal'nego Vostoka* (pp. 76–80). Vladivostok: Izdatel'stvo DVNTs AN SSSR [in Russian].

Oleinikov, A. V., & Oleinikov, N. A. (2005). *Geologia kainozoya srednego Sikhote-Alinya*. Vladivostok: Dal'nauka [in Russian].

Pagani, M., Zachos, J. C., Freeman, K. H., Tipple, B., & Bohany, S. (2005). Marked decline in atmospheric carbon dioxide concentrations during the Paleogene. *Science, 309*, 600–603.

Parfenov, L. M., Badarch, G., Berzin, N. A., Khanchuk, A. I., Kuzmin, M. I., Nokleberg, W. J., Prokopiev, A. V., Ogasawara, M., & Yan, H. (2009). Summary of Northeast Asia geodynamics and tectonics. *Stephan Mueller Spec. Publ. Ser., 4*, 11–33.

Pavlyutkin, B. I. (2007). *The Eocene ust'davydovka flora of the south Primorye*. Vladivostok: Dal'nauka [in Russian].

Pavlyutkin, B. I., Chekryzhov, I. Y., & Petrenko, T. I. (2012). *Geology and flora of lower Miocene in the south Primorye*. Vladivostok: Dal'nauka [in Russian].

Pavlyutkin, B. I., Chekryzhov, I. Y., & Petrenko, T. I. (2014). *Geology and floras of lower Oligocene in the Primorye*. Vladivostok: Dal'nauka [in Russian].

Pavlyutkin, B. I., & Golozubov, V. V. (2010). Paleobotanic evidences for the time of the Sea of Japan origin. *Vestnik Krauntz Nauki o Zemre, 2*, 19–23 [in Russian].

Pavlyutkin, B. I., Nevolina, S. I., Petrenko, T. I., & Kutub-Zade, T. K. (2006). O vozraste paleogenovykh nazimovskoi i khasanskoi svit Yugo-Zapadnogo Primor'ya. *Stratigraphy and Geological Correlation, 14*(3), 116–129 [in Russian].

Pavlyutkin, B. I., & Petrenko, T. I. (1993). Novye materialy po stratigrafii tretichnykh otlozhenii poluostrova Rechnoi (Yuzhnoe Primor'e). *Tikhookeanskaya geologia, 5*, 42–50 [in Russian].

Pavlyutkin, B. I., & Petrenko, T. I. (1994). K stratigrafii tretichnykh uglenosnykh otlozhenii yugo-vostochnoi okrainy Khankaiskogo massiva. *Tikhookeanskaya geologia, 2*, 18–29 [in Russian].

Pavlyutkin, B. I., & Petrenko, T. I. (1997). Problemy stratigrafii tretichnykh obrazovanii poluostrova Pos'et i prilegayutshei territorii (Yugo-Zapadnoe Primor'e). *Tikhookeanskaya geologia, 16*(1), 89–98 [in Russian].

Pavlyutkin, B. I., & Petrenko, T. I. (2010). *Stratigraphy of Paleogene–Neogene sediments in Primorye*. Vladivostok: Dal'nauka [in Russian].

Pearson, P. N., van Dongen, B. E., Nicholas, C. J., Pancost, R. D., Schouten, S., Singano, J. M., & Wade, B. S. (2007). Stable warm tropical climate through the Eocene Epoch. *Geology, 35*, 211–214.

Pearson, P. N., Foster, G. L., & Wade, B. S. (2009). Atmospheric carbon dioxide through the Eocene–Oligocene climate transition. *Nature, 461*, 1110–1113.

Popov, V. K., Maksimov, S. O., Vrzhosek, A. A., & Chubarov, V. M. (2007). Basal'toidy i karbonatitovye tufy Ambinskogo vulkana (Yugo-Zapadnoe Primor'e): geologia i genesis. *Tikhookeanskaya geologia, 26*(4), 75–97 [in Russian].

Popov, V. K., Rasskazov, S. V., Chekryzhov, Y. I., et al. (2005). Kalii-argonovye datirovki i geokhimicheskie kharakteristiki trakhibasal'tov i trakhiandezitov Primor'ya. In N. V. Vladykin (Ed.), *Trudy nauchnoi shkoly "Tshelochnyi magmatizm Zemli"* (pp. 133–135). Moskow: GEOKHI RAN [in Russian].

Popova, S., Utescher, T., Gromyko, D., Bruch, A. A., & Mosbrugger, V. (2012). Palaeoclimate evolution in Siberia and Russian Far East from the Oligocene to Pliocene—Evidence from fruit and seed floras. *Turkish Journal of Earth Sciences, 21*, 315–335.

Qiang, X. K., An, Z. S., Song, Y. G., Chang, H., Sun, Y. B., Liu, W. G., Ao, H., Dong, J. B., Fu, C. F., Wu, F., Lu, F. G., Cai, Y. J., Zhou, W. J., Cao, J. J., Xu, X. W., & Ai, L. (2011). New eolian red clay sequence on the western Chinese Loess Plateau linked to onset of Asian desertification about 25 Ma ago. *Science China Earth Sciences, 54*, 136–144.

Quan, C., Liu, Y. S. C., & Utescher, T. (2011). Paleogene evolution of precipitation in northeastern China supporting the Middle Eocene intensification of the East Asian monsoon. *PALAIOS, 26*, 743–753.

Quan, C., Liu, Y. S. C., & Utescher, T. (2012). Paleogene temperature gradient, seasonal variation and climate evolution of Northeast China. *Palaeogeography, Palaeoclimatology, Palaeoecology, 313–314*, 150–161.

Quan, C., Liu, Z., Utescher, T., Jin, J. H., Shu, J. W., Li, Y. X., & Liu, Y. S. (2014). Revisiting the Paleogene climate pattern of East Asia: A synthetic review. *Earth-Science Reviews, 139*, 213–230.

Quan, C., & Zhang, L. (2005). An analysis of the Early Paleogene climate of the Jiayin area, Heilongjiang province. *Geological Review, 51*, 10–15 [in Chinese with English abstract].

Roth-Nebelsick, A., Utescher, T., Mosbrugger, V., Diester-Haass, L., & Walther, H. (2004). Changes in atmospheric CO_2 concentrations and climate from the late Eocene to early Miocene; paleobotanical reconstruction based on fossil floras from Saxony, Germany. *Paleogeography, Paleoclimatology, Paleoecology, 205*(1–2), 43–67.

Rybalko, V. I., Ovechkin, V. N., & Klimova, R. S. (1980). Kainozoiskie basal'toidy amginskoi serii (Severo-Vostochnoe Primor'e). *Sovetskaya geologia, 12*, 59–71 [in Russian].

Sato, T., Takahashi, N., Miura, S., Fujie, G., Kang, D.-H., Kodaira, S., & Kaneda, Y. (2006). Last stage of the Japan Sea back-arc opening deduced from the seismic velocity structure using wide-angle data. *Geochemistry, Geophysics, Geosystems, 7*, 1–15.

Sokolov, S., Svjseva, O., & Kubli, V. (1977). *Ranges of trees and shrubs of the USSR* (Vol. 1). Leningrad: Nauka [in Russian].

Sokolov, S., Svjseva, O., & Kubli, V. (1980). *Ranges of trees and shrubs of the USSR* (Vol. 2). Leningrad: Nauka [in Russian].

Sokolov, S., Svjseva, O., & Kubli, V. (1986). *Ranges of trees and shrubs of the USSR* (Vol. 3). Leningrad: Nauka [in Russian].

Spicer, R. A. (2017). Tibet, the Himalaya, Asian monsoon and biodiversity—In what ways are they related? *Plant Diversity, 39*, 233–244.

Su, T., Xing, Y. W., Yang, Q. S., & Zhou, Z. K. (2009). Reconstructions of mean annual temperature in Chinese Eocene Paleofloras based on leaf margin analysis. *Acta Palaeontologica Sinica, 48*, 65–72.

Sun, X., & Wang, P. (2005). How old is the Asian monsoon system? Palaeobotanical records from China. *Palaeogeography, Palaeoclimatology, Palaeoecology, 222*, 181–222.

Tada, R., Zheng, H. B., & Clift, P. O. (2016). Evolution and variability of the Asian monsoon and its potential linkage with uplift of the Himalaya and Tibetan Plateau. *Progress in Earth and Planetary Science, 3*(4), 1–26. https://doi.org/10.1186/s40645-016-0080-y.

Takaya, K., & Nakamura, H. (2005). Mechanism of intraseasonal amplification of the cold Siberian high. *Journal of the Atmospheric Sciences, 62*, 4423–4440.

Tashchi, S. M., Ablaev, A. G., & Mel'nikov, N. G. (1996). *Kainozoiskii bassein Zapadnogo Primor'ya i sopredel'nykh territorii Kitaya i Korei*. Vladivostok: Dal'nauka [in Russian].

Ushimura, H., Kono, M., Tsunakawa, H., Kimura, G., Wei, Q., Hao, T., & Liu, H. (1996). Paleomagnetism of Late Mezosoic rocks from northeastern China: The role of the Tan-Lu fault in the North China Block. *Tectonophysics, 262*, 301–319.

Utescher, T., Ashraf, A. R., Dreist, A., Dybkjær, K., Mosbrugger, V., Pross, J., & Wilde, V. (2012). Variability of Neogene continental climates in Northwest Europe—A detailed study based on microfloras. *Turkish Journal of Earth Sciences, 21*, 289–314.

Utescher, T., Bondarenko, O. V., & Mosbrugger, V. (2015). The Cenozoic cooling—Continental signals from the Atlantic and Pacific side of Eurasia. *Earth and Planetary Science Letters, 415*, 121–133.

Utescher, T., Bruch, A. A., Erdei, B., François, L., Ivanov, D., Jacques, F. M. B., Kern, A. K., Liu, (. Y. S.). C., Mosbrugger, V., & Spicer, R. A.

(2014). The coexistence approach—Theoretical background and practical considerations of using plant fossils for climate quantification. *Palaeogeography, Palaeoclimatology, Palaeoecology, 410*, 58–73.

Utescher, T., Bruch, A. A., Micheels, A., Mosbrugger, V., & Popova, S. (2011). Cenozoic climate gradients in Eurasia—A palaeo-perspective on future climate change? *Palaeogeography, Palaeoclimatology, Palaeoecology, 304*, 351–358.

Utescher, T., Djordjevic-Milutinovic, D., Bruch, A. A., & Mosbrugger, V. (2007). Palaeoclimate and vegetation change in Serbia during the last 30 Ma. *Palaeogeography, Palaeoclimatology, Palaeoecology, 253*, 141–152.

Utescher, T., & Mosbrugger, V. (2007). Eocene vegetation patterns reconstructed from plant diversity—A global perspectives. *Palaeogeography, Palaeoclimatology, Palaeoecology, 247*, 243–271.

Utescher, T., & Mosbrugger, V. (2018). The Palaeoflora database. www.palaeoflora.de.

Utescher, T., Mosbrugger, V., Ivanov, D., & Dilcher, D. L. (2009). Present-day climatic equivalents of European Cenozoic climates. *Earth and Planetary Science Letters, 284*(3–4), 544–552.

Varnavskii, V. G., Sedykh, A. K., & Rybalko, V. I. (1988). *Paleogen i neogen Priamur'ya i Primor'ya*. Vladivostok: Izdatel'stvo DVO AN SSSR [in Russian].

Verkhovskaya, N. B., & Kundyshev, A. S. (1989). Fisionomicheskie osobennosti sporovo-pyl'tsevykh spektrov i ikh ispol'zovanie v stratigrafii. In V. A. Krassilov & R. S. Klimova (Eds.), *Kainozoi Dal'nego Vostoka* (pp. 128–134). Vladivostok: Izdatel'stvo DVO AN SSSR [in Russian].

Wang, Q., Ferguson, D. K., Feng, G. P., Ablaev, A. G., Wang, Y. F., Yang, J., Li, Y. L., & Li, C. S. (2010). Climatic change during the Palaeocene to Eocene based on fossil plants from Fushun, China. *Palaeogeography, Palaeoclimatology, Palaeoecology, 295*, 323–331.

Wang, B., Liu, J., Kim, H. J., Webster, P. J., Yim, S. Y., & Xiang, B. (2013). Northern hemisphere summer monsoon intensified by mega-El Nino/southern oscillation and Atlantic multidecadal oscillation. *Proceedings of the National Academy of Sciences, 110*, 5347–5352.

Wang, C. S., Dai, J., Zhao, X., Li, Y., Graham, S. A., He, D., Ran, B., & Meng, J. (2014a). Outward-growth of the Tibetan Plateau during the Cenozoic: A review. *Tectonophysics, 621*, 1–43.

Wang, P. X., Wang, B., Cheng, H., Fasullo, J., Guo, Z. T., Kiefer, T., & Liu, Z. Y. (2014b). The global monsoon across timescales: Coherent variability of regional monsoons. *Climate of the Past, 10*, 2007–2052.

Wilf, P. (2000). Late Paleocene-early Eocene climate changes in southwestern Wyoming: Paleobotanical analysis. *Geological Society of America Bulletin, 112*, 292–307.

Wing, S. L., & Harrington, G. J. (2001). Floral response to rapid warming in the earliest Eocene and implications for concurrent faunal change. *Paleobiology, 27*, 539–563.

Wing, S. L., Harrington, G. J., Smith, F. A., Bloch, J. I., Boyer, D. M., & Freeman, K. H. (2005). Transient floral change and rapid global warming at the Paleocene–Eocene boundary. *Science, 310*, 993–996.

Wu, Z.Y., & Raven, P.H. (Eds.) (1999). *Flora of China*. vol. 4 (Cycadaceae through Fagaceae). Beijing and St. Louis: Science Press and Missouri Botanical Garden.

Xiao, G. Q., Abels, H. A., Yao, Z., Dupont-Nivet, G., & Hilgen, F. J. (2010). Asian aridification linked to the first step of the Eocene–Oligocene climate transition (EOT) in obliquity-dominated terrestrial records (Xining Basin, China). *Climate of the Past, 6*, 501–513.

Yamamoto, T., & Hoang, N. (2009). Synchronous Japan Sea opening Miocene fore-arc volcanism in the Abukuma Mountains, NE Japan: An advancing hot asthenosphere flow versus Pacific stab melting. *Lithos, 112*, 575–590.

Yanovskaya, N. M. (1954). Novyi rod Embolotheriidae iz paleogena Mongolii. Tretichnye mlekopitayutshie. *Trudy PIN AN SSSR, 55*(3), 5–43 (in Russian).

Zachos, J. C., Dickens, G. R., & Zeebe, R. E. (2008). An Early Cenozoic perspective on greenhouse warming and carbon-cycle dynamics. *Nature, 451*, 279–283.

Zhang, S. P., & Wang, B. (2008). Global monsoon summer rainy seasons. *International Journal of Climatology, 28*, 1563–1578.

Zhu Z.W. (1993). *Paleomagnetism in eastern China and the horizontal displacement of the Tancheng-Lujiang fault zone*. In J.W. Xu (Ed.), Tancheng-Lujiang Wrench Fault System. John Wiley et Sons.